



Mira Dreier, BSc

*Evaluation of Adjustable Loop Suspensory Anterior Cruciate Ligament
Fixation Devices*

MASTER'S THESIS

to achieve the university degree of

Diplom-Ingenieurin

Master's degree programme: Biomedical Engineering

submitted to

Graz University of Technology

Supervisor:

Assoc.Prof. Dipl.-Ing. Dr.techn. Jörg Schröttner

*Institute of Health Care Engineering with European Testing
Center of Medical Devices*

Graz, April 2019

EIDESSTATTLICHE ERKLÄRUNG

AFFIDAVIT

Ich erkläre an Eides statt, dass ich die vorliegende Arbeit selbstständig verfasst, andere als die angegebenen Quellen/Hilfsmittel nicht benutzt, und die den benutzten Quellen wörtlich und inhaltlich entnommenen Stellen als solche kenntlich gemacht habe. Das in TUGRAZonline hochgeladene Textdokument ist mit der vorliegenden Masterarbeit/Diplomarbeit/Dissertation identisch.

I declare that I have authored this thesis independently, that I have not used other than the declared sources/resources, and that I have explicitly indicated all material which has been quoted either literally or by content from the sources used. The text document uploaded to TUGRAZonline is identical to the present master's thesis/diploma thesis/doctoral dissertation.

Datum / Date

Unterschrift / Signature

Die Technische Universität Graz übernimmt mit der Betreuung und Bewertung einer Masterarbeit keine Haftung für die erarbeiteten Ergebnisse: Eine positive Bewertung und Anerkennung (Approbation) einer Arbeit bescheinigt nicht notwendigerweise die vollständige Richtigkeit der Ergebnisse.

Acknowledgements

Firstly, I would like to thank my family and friends for their continuous support and love. Thank you MaPa for supporting me wherever I want to go and for believing in me no matter what. I would also like to thank Dr. Lisa and her lovely Mr. Chris for being there for me with sisterly advice and unconditional support. Finally, I want to thank Jacob for always supporting me and making me smile, even when through my eyes everything seems impossible.

Furthermore, I would like to thank the director of the research department of Arthrex Dr. Coen Wijdicks and the biomechanical research supervisor Martina Roth, M.Sc. for giving me the opportunity to join their team and work in such a professional environment. I would also like to thank Dipl.-Ing. Samuel Bachmaier for his continuous support and guidance during this thesis.

Moreover, I would like to thank the whole research team for making my time at Arthrex so special. Especially I want to thank Marina for helping with any problem that occurred during my thesis and Max, Maxi, Franzi and Dani for their invaluable assistance with the preparation of the specimen.

Last but not least, I would like to express my gratitude to my supervisor Assoc. Prof. Dipl.-Ing. Dr. techn. Jörg Schröttner, member of the Institute of Health Care Engineering at Graz University of Technology for the opportunity to write my master's thesis dealing with such an interesting and thrilling topic at Arthrex GmbH.

Untersuchung von einstellbaren Kortikalisfixierungsimplantaten zur Verankerung des vorderen Kreuzbandes

Zusammenfassung

Ein einstellbares Kortikalisfixierungsimplantat (Abk. engl.: ALD) kann bei der Rekonstruktion des vorderen Kreuzbandes im menschlichen Knie zur Verankerung verwendet werden. Im Rahmen dieser Studie wird der Entwicklungsprozess des ALD *TightRope II* von Arthrex analysiert. Dieser umfasst eine Klassifizierung nach der neuen Medizinprodukteverordnung (MDR) und eine Analyse möglicher Wege für die Konformitätsbewertung nach der MDR. Des Weiteren werden die biomechanischen Eigenschaften von häufig verwendeten ALDs in mehreren Labortests untersucht, mit dem Ziel ein standardisiertes Testverfahren zu entwickeln. Die Tests zeigen große Unterschiede im Zugverhalten und der Stabilität der verschiedenen ALDs, welche auf das jeweilige Design zurückzuführen sind.

Schlüsselwörter: Kreuzbandrekonstruktion, einstellbares Kortikalisfixationsimplantat, Medizinprodukteverordnung, Entwicklungsprozess, biomechanische Tests

Evaluation of Adjustable Loop Suspensory Anterior Cruciate Ligament Fixation Devices

Abstract

An adjustable loop device (ALD) can be used for the cortical fixation upon reconstructing the anterior cruciate ligament (ACL) in the human knee. In this study the development process of the ALD *TightRope II* from Arthrex is analyzed. Within this process the device is classified according to the new medical device regulation (MDR) and possible ways for the conformity assessments according to the MDR are investigated. Furthermore, a comprehensive controlled laboratory investigation is included in this study to examine the biomechanical properties of commonly used cortical fixation devices, with the aim of implementing a standard testing procedure for adjustable loop devices. The tests reveal great differences between the ALDs regarding the tensioning behavior and stability. Those differences occur due to the different designs of the ALDs.

Keywords: anterior cruciate ligament reconstruction, adjustable loop device, medical device regulation, development process, biomechanical testing

List of Abbreviations

ACL	anterior cruciate ligament
AIMD	active implantable medical device
ALD	adjustable loop device
AM	anteromedial
CFT	chinese finger trap
CT	computer assisted tomography
DTM	design traceability matrix
FLD	fixed loop device
IVDR	in vitro diagnostic regulation
LCL	lateral collateral ligament
MCL	medial collateral ligament
MDD	medical device directive
MDR	medical device regulation
MRI	magnetic resonance imaging
PCL	posterior cruciate ligament
PET	polyethylene terephthalate (polyester)
PL	posterolateral
QMS	quality management system
SD	standard deviation
UHMWPE	ultra-high molecular weight polyethylene
US	ultra sound

Table of Contents

EIDESSTÄTTLICHE ERKLÄRUNG.....	I
Acknowledgements	II
Zusammenfassung	III
Abstract	III
List of Abbreviations	IV
1. Introduction	1
1.1. Anatomy of the Knee	2
1.2. Biomechanical Environment of the Knee.....	6
1.2.1. Kinematics of the ACL	7
1.3. ACL Injuries.....	8
1.3.1. Diagnosis of ACL Tears	9
1.4. Treatment Options & State of the Art.....	10
1.5. Application of an Adjustable Loop Device	14
1.6. Analysis of the Development Process of a Medical Device	16
2. Aim of this Thesis	19
3. Materials and Methods	20
3.1. Development Process of <i>TightRope II</i>	20
3.2. Evaluation of Different ALD Designs	21
3.2.1. Transmission Ratio	22
3.2.2. Operating Mechanism.....	23
3.2.3. Locking Mechanism	24
3.3. Test Methods and Setup	25
3.3.1. ALD Loop Shortening Test.....	25
3.3.2. ALD Stability Test	29
3.3.2.1. Single Device Test	30
3.3.2.2. Device -Tendon Test	31
3.4. Data Analysis.....	34

3.4.1.	ALD Loop Shortening Test.....	34
3.4.2.	ALD Stability Test	36
4.	Results	37
4.1.	Development Process <i>TightRope II</i>	37
4.1.1.	Classification of <i>TightRope II</i>	39
4.1.2.	Conformity Assessment	40
4.1.2.1.	MDR Annex IX.....	41
4.1.2.2.	MDR Annex X & XI.....	43
4.2.	Pre-Testing of <i>Polished</i> and <i>Non-Polished TightRope II</i> Buttons	44
4.2.1.	Loop Shortening Test.....	45
4.2.2.	Stability Test - Single Device	46
4.3.	ALD Loop Shortening	46
4.4.	ALD Stability Test.....	50
5.	Discussion	57
6.	Conclusion	62
	Literature	63
	Figures	67
	Tables	70
	Appendix	A

1. Introduction

Along with increasing enthusiasm for sports comes an increase of sport related injuries. One of the most common injuries in the human knee is the tear of the anterior cruciate ligament (ACL) [1-4]. Mall et al. [5] reported about 200,000 ACL injuries and 100,000 to 150,000 ACL reconstructions per year in the United States of America, while Wildhalm [3] recorded 8,103 reconstructions in Austria in 2014. Athletes practicing sports like skiing, soccer, tennis, squash, and volleyball are likely to hurt their ACL due to a prompt change of direction, fast stop and go movements, landing incorrectly from a jump or even due to a direct contact or collision [1, 6, 7]. Since the tear of the ACL generally occurs as a sport injury, mainly young people are affected [3].

There are many ways to treat an ACL injury, including the operative reconstruction, which is considered as the gold standard especially for young active patients who wish to return to active sports as fast as possible. During the reconstruction, the remaining parts of the ligament are removed and an allograft or autograft from either the hamstring or patella tendon is implanted in order to substitute the ACL. [1, 8] The implanted graft can be attached to the femur and tibia with for example a metal or bio-interference screw, a dissolving bioscrew, a biodegradable or metal pin, a fixed loop device or an adjustable loop device (ALD) [4].

This work describes the development process and the possible conformity assessment procedures according to the MDR of the new adjustable loop device developed by Arthrex Inc. (Naples, Florida). This new product is called *TightRope II* and is an improved version of the *TightRope*, which is currently on the market.

Barrow et al. [9] and Ahmad et al. [10] performed biomechanical stability tests with some common ALDs including the *Tight Rope*. For the cyclic testing, they defined an irreversible elongation of 3 mm as clinical failure. In both studies, *TightRope* reached clinical failure, after fewer cycles than other comparable products.

Since the locking mechanism of *TightRope II* is substantially different from that of *TightRope*, the described disadvantage is likely to be removed. In order to verify that, this thesis evaluates the most important ALDs on the market based on biomechanical testing methods. In these methods all main aspects of ALDs will be assessed, with the goal of implementing a standard evaluation method.

1.1. Anatomy of the Knee

Since a profound knowledge about the structures in the knee is of great importance, the anatomy of the knee is discussed in this chapter.

The knee joint also known as, *articulatio genus* is a pivot joint, which allows flexion and extension as well as rotation in the flexed position [11]. It is the biggest joint in the human body and divided into two joints: the articulation femorotibialis, located between femur and tibia and the articulation femoropatellaris, between femur and patella [12]. The knee joint consists of bones and different soft tissues such as muscles, ligaments, tendons, cartilage, capsule ribbon structure, and menisci [13].

In Figure 1 the three bones of the knee joint femur, tibia and patella are shown. Both femur and tibia have a *condylus medialis* and a *condylus lateralis*, which build the joint hinges and are located at the distal end of the femur and at the proximal end of the tibia [11]. The two condyles of the tibia are interrupted by the *eminentia intercondylaris*, which is separated into the *tuberculum intercondylare mediale* and the *tuberculum intercondylare laterale* (see Figure 1 B).

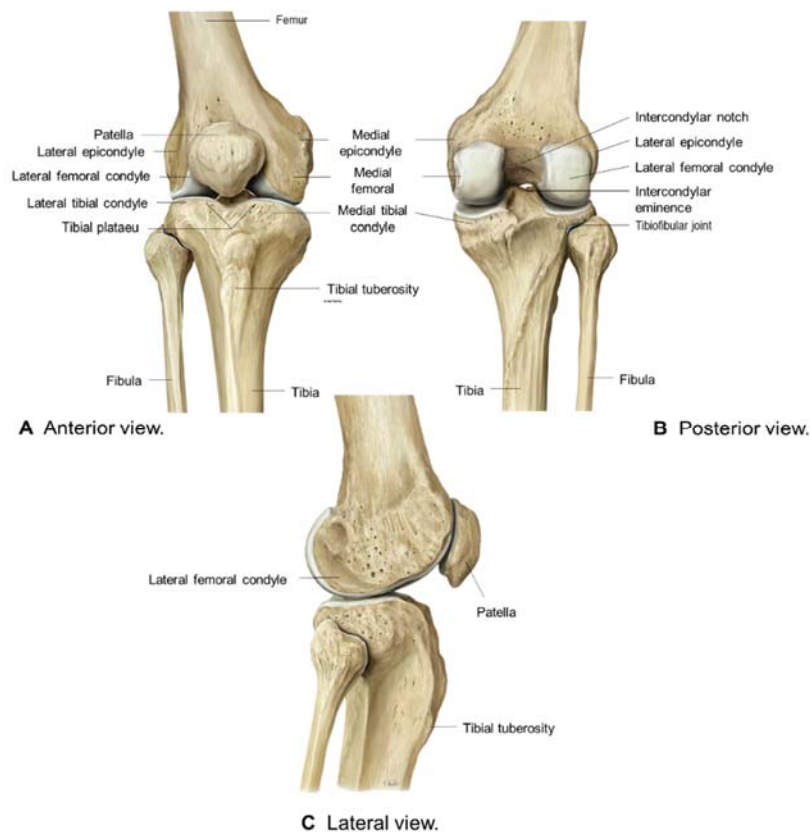


Figure 1: Anatomy of the bones of the right knee: Anterior view (A), posterior view (B) and lateral view (C). The figure has been modified from ref. [6].

The patella is the biggest sesamoid bone in the human body. As illustrated in Figure 2 the patella is embedded in the quadriceps tendon, which is united with the patellar tendon. [6] The osseous structures described above have a low elasticity and mainly absorb compression forces [13].

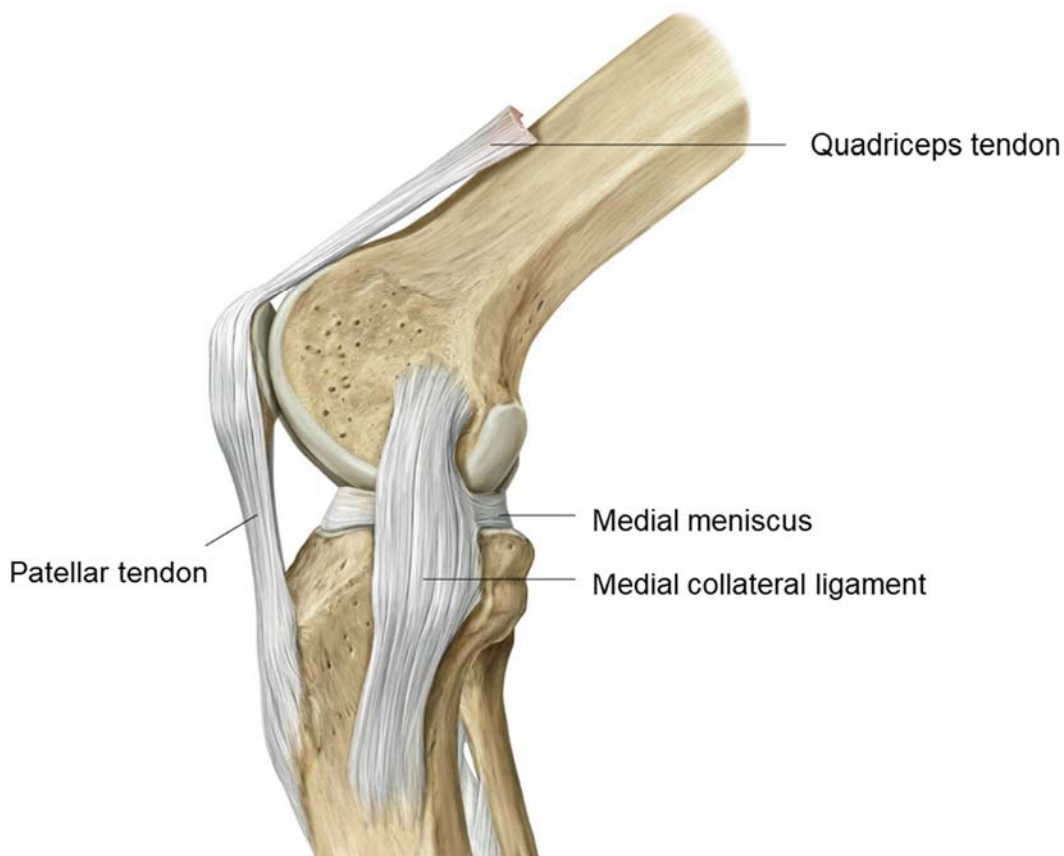


Figure 2: Medial view of the knee joint. The figure has been modified from ref. [6].

The surfaces of femur and tibia are connected via two menisci and the hyaline cartilage, which covers the surface of the joint hinge. The primary task of the menisci is the weight distribution at a stressed knee joint in order to reduce selective contact stress. In addition to that, they increase the stability of the knee joint and control passive movement, as they restrict hyperextension and hyperflexion. Both menisci, the external one (meniscus lateralis) and the inner one (meniscus medialis), are wedge shaped and composed of connective tissue and collagen drums. [11-13]

Even though the outer parts of the menisci are connected to the membrane synoviales and the capsula articularis they are displaceable over the tibia. While the meniscus medialis is crescent shaped and connected to the medial collateral ligament, the

meniscus lateralis is nearly circle shaped and not connected to the lateral collateral ligament (see Figure 3). [11-13]

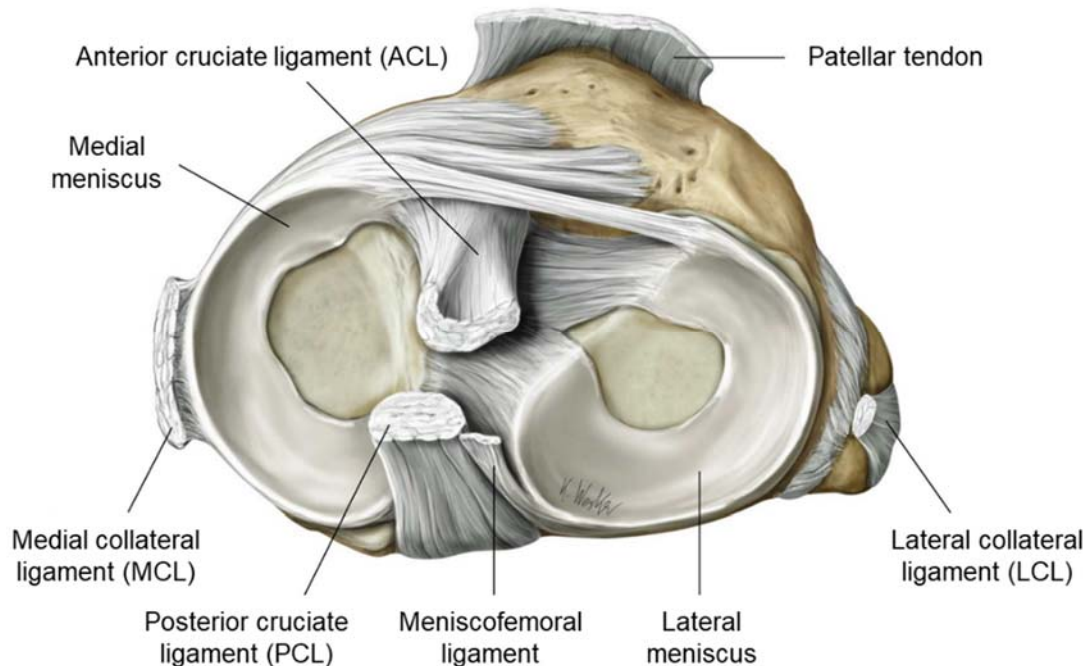


Figure 3: Tibia-plateau with meniscus medialis and lateralis. The figure has been modified from ref. [6].

In addition to the components already mentioned above the knee joint consists of two ligament systems: the collateral ligaments, (medial and lateral) and the cruciate ligaments (anterior and posterior) [12].

The collateral ligaments are placed on the outside of the joint between femur and tibia (see Figure 4). They are connective tissue that is rich in water and collagen, with a small amount of elastin. The collateral ligaments guide the bending and stretching movement and restrict the rotation of the knee during extension, thus protecting it against varus and valgus stress. The medial collateral ligament (MCL) starts at the medial femoral epicondyle and reaches up to the medial face of the tibia, whereas the lateral collateral ligament (LCL) extends from the lateral femoral epicondyle to the head of the fibula. While the MCL is tightly bound to the medial meniscus, the LCL is not connected to the meniscus. [13, 14]

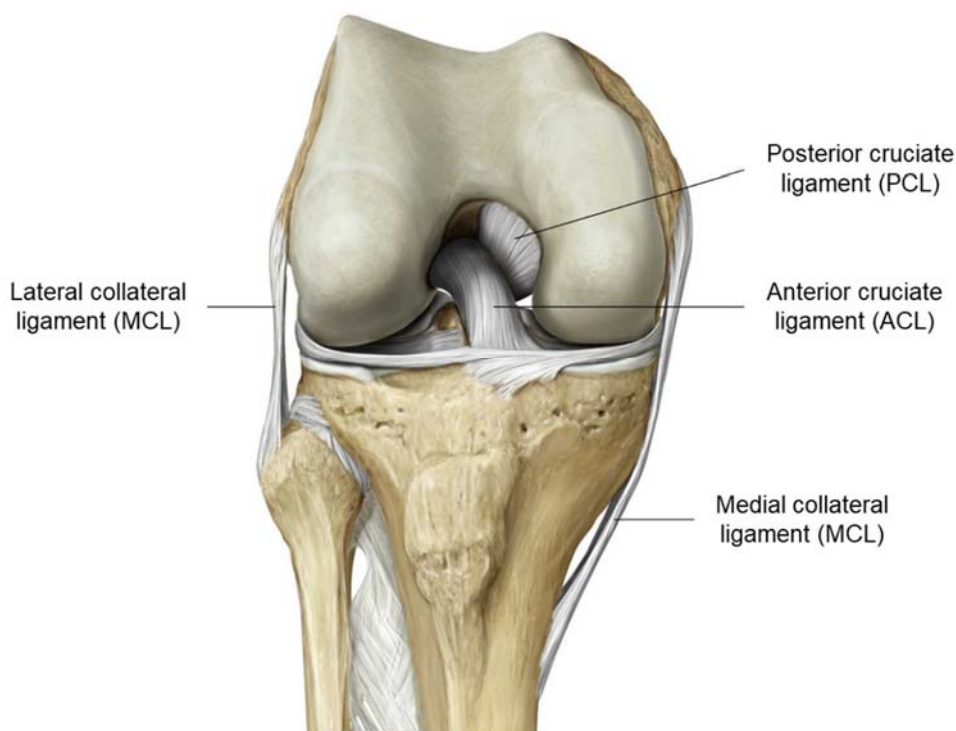


Figure 4: Schematic of the collateral and cruciate ligaments. The figure has been modified from ref. [6].

The anterior cruciate ligament (ACL) extends from the back of the lateral femur condyle to the medial part of the tibia and is divided into two bundles, the anteromedial (AM) and the posterolateral (PL) bundle. The AM and the PL bundles do not have an identical isometry during movement. While extended, the two bundles are parallel but as the bending angle increases, the AM bundle moves backwards and experiences tension while the PL bundle moves forward and begins to relax. [15] The posterior cruciate ligament (PCL) is stronger than the anterior one and reaches diagonally from the lateral surface of the medial femur condyle to the external site of the lateral tibia condyle [11]. The PCL has a length and width of approximately 38 mm and 13 mm, respectively, while the ACL measures roughly 30 mm in length and approximately 11 mm in width. Therefore, the ACL ruptures more frequently. [16, 17]

Due to their position, the cruciate ligaments cross and rotate around each other while flexing and extending the knee joint. Their main task is to stabilize the knee and to keep the hinge bodies in a fixed position relative to each other. Therefore, one of the two ligaments is always under tension. Concerning the stability of the knee, the ACL prevents the tibia from a subluxation towards the front, while the PCL prevents the tibia

plateau from a subluxation in a dorsal direction. Additionally, the ACL protects from inner rotation and maximal outer rotation in a flexed position. [6, 12, 13, 15]

Another task covered by the cruciate ligaments is the proprioception, which is the ability to sense inner motions of the knee joint due to neuro receptors at the ligaments. Therefore, the ACL and the PCL have a rich sensory innervation. Receptors can collect valuable information about static and kinesthetic perception, which ensures a high sensibility and thus safety of the knee. [14, 18]

1.2. Biomechanical Environment of the Knee

As mentioned above, the knee joint is divided into the patellofemoral joint, which is a sliding contact bearing and the tibiofemoral joint. The tibiofemoral joint is a combination of a hinge joint and a rotational joint. [14] This combination allows flexion and extension in the sagittal plane as well as inward and outward rotation about the longitudinal axis of the tibia while the joint is in a flexed position. During extension and flexion, the femur is rolling and sliding on the tibial plateau. This movement is supported by the menisci, the synovial fluid, and cartilage, which minimize the friction. [19] Figure 5 shows five different positions of the tibiofemoral joint during the natural movement process. In the initial position the joint is in full extension, this position is commonly defined as 0 degrees. The contact points on femur and tibia are marked red in Figure 5. During flexion of the joint those contact points move backward, due to a combination of rolling and gliding between the two bones. [20, 21]

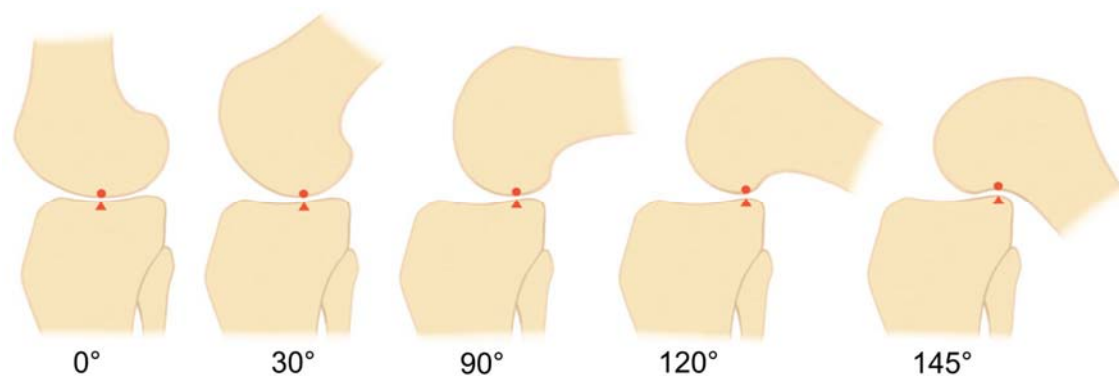


Figure 5: Schematic drawing of the flexion process and the according movement between femur and tibia. The figure has been modified from ref. [20].

The two condyles of the knee joint are moving differently during flexion. This is caused by the unequal distribution of rolling and gliding movement between the medial and lateral condyle (see Figure 6). As the medial condyle is mainly gliding on the tibia, its center of rotation remains nearly in the same position. In contrast, the lateral condyle is rolling more on the tibia, therefore its center of rotation moves backwards during flexion. [21]

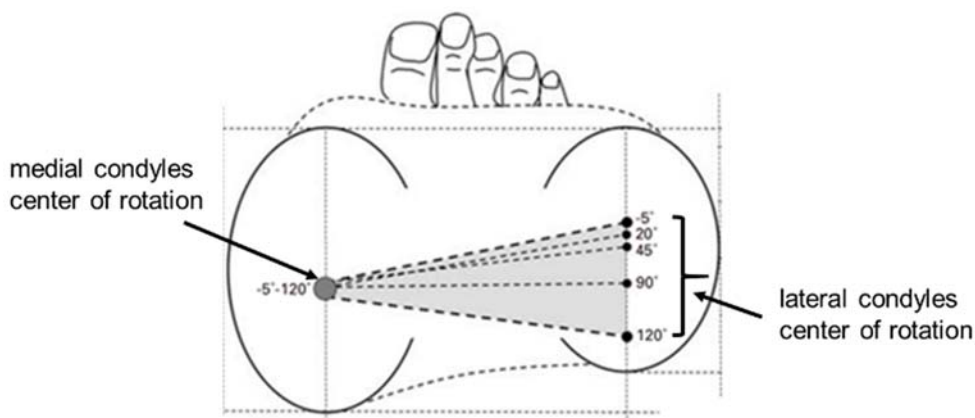


Figure 6: Schematic of the tibial plateau from above. The change of the center of rotation of the femoral condyles during flexion of the knee is indicated. The lateral condyle performs a “roll-back” motion, while the medial condyle rotates around the same horizontal axis. This image has been modified from ref.[21].

1.2.1. Kinematics of the ACL

The anterior cruciate ligament has elastic properties and shows a low initial stiffness at low strains. With an increase of strain a linear elastic behavior occurs until the ultimate failure load, where the ACL tears, is reached. [22] Several studies have shown that the length of the ACL decreases with an increasing flexion angle of the knee joint [17, 23, 24]. Li et al. [17] investigated the ACL's behavior during weight bearing and reported an average length of the ACL of roughly 30 mm at full extension and around 27 mm at 90° flexion. This 3 mm difference in length corresponds to a 10 % decrease, which is similar to the results reported by Taylor et al. [24]. The mentioned mechanical values and the ACL function zone, defined by Bachmaier et al. [25], are sketched in Figure 7. A second x-axis shows the flexion of the knee in degrees, hereby zero degrees correspond to full extension. It can be seen, that the ACL starts to experience tension at around 30 degrees, which already occurs during light activities such as walking [23].

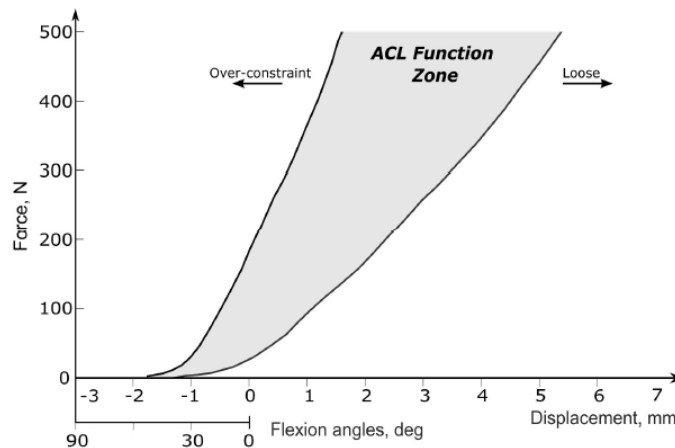


Figure 7: Schematic of the displacement of the ACL as function of force applied to it, including the over-constraint and loose regions. This figure has been adapted from ref. [25].

1.3. ACL Injuries

In order to provide an overview of the different types of ACL injuries, they are discussed within this chapter. As stated before, the tear of the ACL mainly occurs as a sport related injury. Particularly while performing high demand sports such as skiing, soccer, tennis, squash, and volleyball, the risk is enormous. [1, 6, 7, 26] The principal causes for a tear of the ACL are the combination of loaded or unloaded varus/valgus flexion, in combination with rotation, hyperextension or hyperflexion [27]. A major symptom of an ACL rupture is the loss of stability in the knee joint, specifically during movement. As a consequence of leaving these injuries untreated progressive degenerative lesions and sub-sequent injuries may occur and can lead to the development of arthritis in the long term. [28, 29]

According to Sherman et al. [30], who investigated ACL tears in 50 patients, ACL tears can be classified into four different types, depending on their location between femur and tibia. Type 1 tears are true soft-tissue avulsions with minimal ligament tissue left on the femur. The remaining categories, type 2-4 indicate how much tissue is left on the femur. While in type 2 ruptures there are up to 20 % of the tissue left on the femur, type 3 and 4 indicate the remainder of up to 33 % and 50 % of tissue, respectively (see Figure 8). Of the investigated 50 patients, 26 % had a type 1 tear, 30 % suffered type 2 tears and 22 % experienced type 3 and type 4 tears, respectively. Surprisingly, the incidence rate in women is three times higher than that in men. A reason for that may

be that women have increased quadriceps angles and increased posterior tibial slopes. [31]

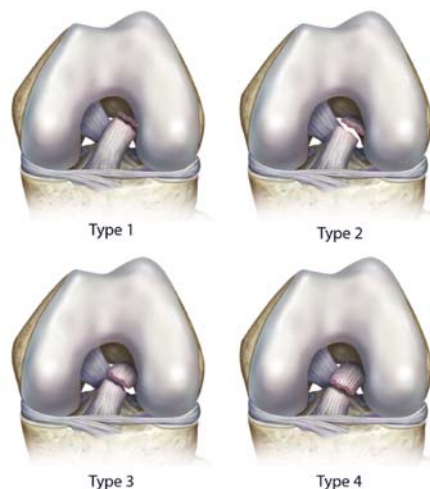


Figure 8: ACL tear type classification by Sherman et al. This figure has been modified from ref. [32].

1.3.1. Diagnosis of ACL Tears

There are two main ways to diagnose an ACL rupture, the imaging process and the clinical examination. To diagnose a knee injury the following imaging procedures can be performed: X-ray spectroscopy, magnetic resonance imaging (MRI), a computer assisted tomography (CT) or an ultrasound (US). Since an MRI is the best option to visualize soft tissue, it is the most commonly used imaging procedure. [27, 33] Within the clinical examination, the range of motion and the stability are analyzed. During a stability test, the displacement range of the joint parts relative to each other is measured in millimeters. Examples for clinical examination methods are the Lachman test, the pivot shift test and the drawer test. [3, 27, 28] Previous studies have shown that the Lachman test is the most sensitive test method, while the pivot shift test is the most specific method [34-36]. In the following paragraphs, the three clinical examination methods are described briefly.

With the Lachman test, the displacement distance between tibia and femur is evaluated. For that purpose, the knee is placed in a flexed position at an angle of roughly 20° - 30°. The heel touches the ground and the lower leg is moved abruptly in an anterior direction. When there is no solid stop perceptible it is likely that the ACL is ruptured. [27]

While the knee is slightly bent during the Lachman-test, the patient is lying on their back with the leg stretched for the pivot shift test. The femur is then fixed while an inner rotation and abduction is performed. Subsequently, the knee is bent slowly. If the ACL is ruptured, the tibia subluxates toward an anterior position during this test. [14]

A third possible clinical examination method is the so-called drawer test. It is performed while the patient is lying on their back, the knee is 90° flexed and the foot is laid up on a table. In order to evaluate the possible displacement range of femur and tibia relative to each other, the tibia head is moved anteriorly and posteriorly. [27]

1.4. Treatment Options & State of the Art

As there are various types of possible ACL ruptures and every human body is unique, there are numerous available methods for treating such an injury. Those methods will be presented in this chapter. An ACL injury can be treated either operatively or conservatively; The operative treatment is further divided into repair and reconstruction. Within the reconstruction, an autograft or allograft can be used to replace the ACL (see Figure 9).

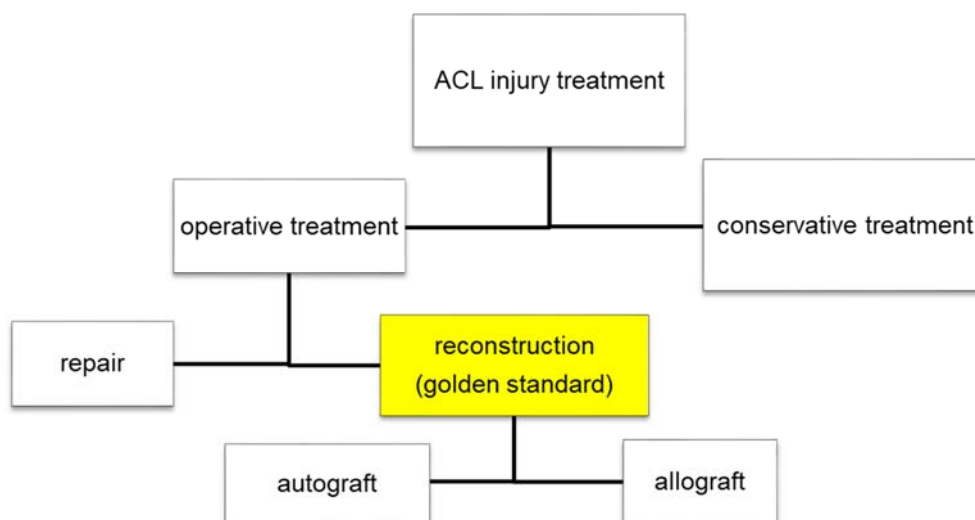


Figure 9: Possible treatments for an ACL injury.

For the decision, whether a conservative treatment or a surgical treatment is more suitable, the following factors are essential: the patient's age and activity level, the instability of the knee joint as well as any additional disease such as for example diabetes mellitus [3, 28, 37].

Voigt et al. [38] and Delincé et al. [39] reported that a conservative treatment is a valid option for elderly patients and for those without a high activity level, since the standard risk factors of an operation can be avoided with the conservative treatment. Although it has to be considered that the risk of later damage to the meniscus increases [37]. Young active patients, who wish to return to high-risk pivoting sports as soon as possible, are usually treated surgically [1, 8, 28, 40]. The mechanical instability is an indication for the surgical treatment in order to prevent the knee from further meniscal or cartilage damage [28, 37]. Another indication for the operative treatment is that about 75% of the injuries are non-isolated injuries, which means that the tear of the ACL is not the only damage in the knee. Typical concomitant injuries are multi-ligament injuries, traumatic cartilage lesion and meniscus damage. [37]

The historically most often used operative treatment is the repair. In such a treatment, the two ends of the original ACL are re-approximated to each other with a suture. This has been one of the earliest methods used for treating an ACL tear. However, several studies have shown poor outcome of the repair, as the ACL does not heal properly. Therefore, the repair has been almost completely replaced by the reconstruction. [8, 40]

The reconstruction of the ACL is seen as the gold standard [1, 8, 28, 40]. In this method, the remaining parts of the ligament are removed and replaced by an autograft or allograft. While the ligament is taken from the patients themselves for an autograft, an allograft comes from a dead human donor. [1] Using an allograft has the advantage of decreased surgical time and no additional pain or scar on the donor site. However, the risk of infection and low grade immune rejection as well as delayed incorporation is higher [4]. There are various options for reconstruction using an implanted autograft. As presented in Figure 10, either parts of the hamstring tendon, the middle third of the patella tendon, or a quad-patella-bone can be used as graft. [41]

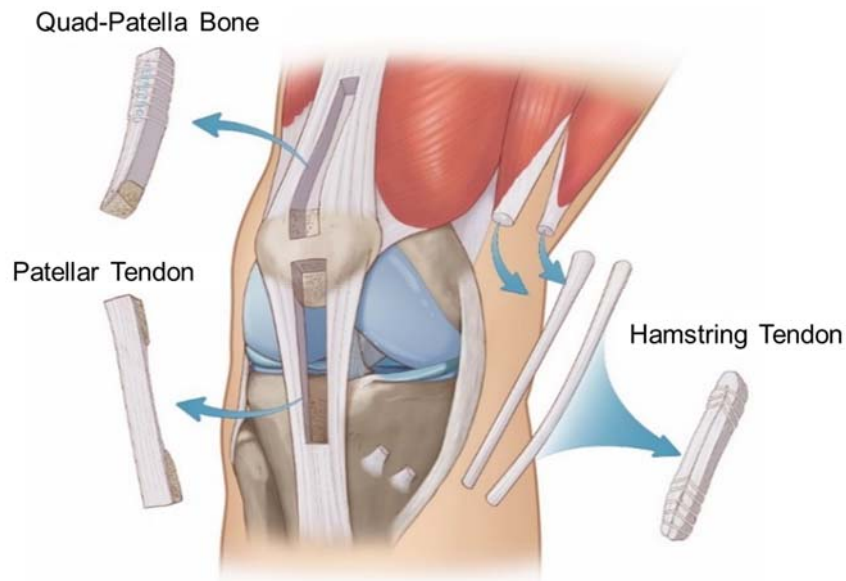


Figure 10: Autograft options for an ACL reconstruction. This image has been modified from ref. [41].

The decision which autograft is used has a high impact on the patient. The healing process is different depending on whether the graft consists only of a tendon or a tendon bone combination. Furthermore, the pain at the location of extraction is not the same for all three options. In Table 1 the advantages and disadvantages of each autograft are summarized. [4]

Table 1: Advantages and disadvantages of autografts. This table has been adapted from ref. [4].

type	Patellar Tendon	Hamstring	Quadriceps
advantage	<i>Strongest healing method</i>	<i>Small incision & less painful harvest</i>	<i>Rare sensory loss</i>
	<i>Quicker healing process</i>	<i>Less problem with knee pain</i>	<i>Thicker cross sectional area than bone-tendon bone grafts</i>
disadvantage	<i>Pain in donor site</i>	<i>Slower healing process for soft tissue-to-bone</i>	
	<i>Large incision</i>	<i>Harvest is technical demanding</i>	<i>Q-muscle atrophy</i>
	<i>Possibility of patella fracture</i>	<i>Diffuse multiligamentous laxity</i>	<i>Violation of extensor mechanism</i>

Since the ACL has two bundles (AM & PM) there are two methods used for the reconstruction. The single bundle technique and the double bundle technique. As described previously, the ACL is not isometric and the tasks of the two bundles are different. The anteromedial bundle affects the knee's anterior stability, while the posterolateral bundle is relevant for rotary stability. [38]

In the double bundle technique, two tunnels are drilled into femur and tibia, respectively and a graft is inserted into each tunnel (see Figure 11). On the other hand, in the single bundle technique there is only one tunnel drilled into femur and tibia, respectively. Xu et al. [42] investigated the outcomes of both techniques and reported a better anterior and rotational stability for the double bundle technique. However, there is no significant difference in patient's satisfactory rates in long-term results. The operation time in the single bundle technique is shorter and there is less bone loss since there is only one tunnel drilled into the bone. Therefore, the single bundle technique is the standard method. [38, 43]

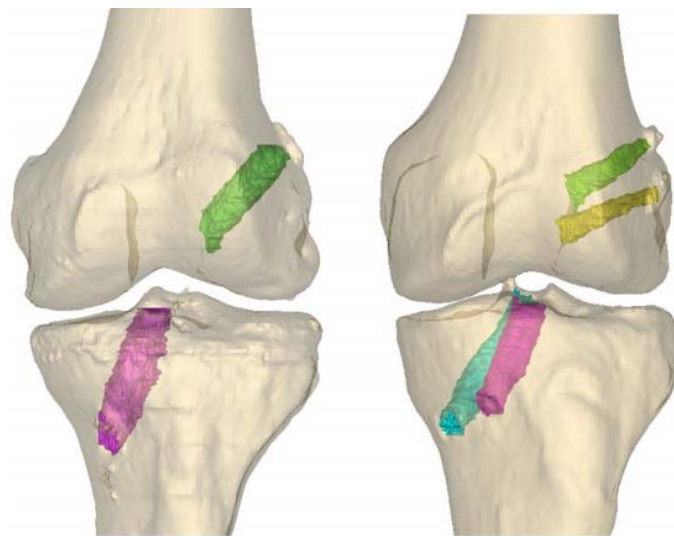


Figure 11: 3D CT model of single bundle technique (left) and double bundle technique (right). This figure has been modified from ref. [43].

The fixation of the graft is essential for a successful reconstruction. For an early rehabilitation, the fixation has to be strong in order to avoid movement of the inserted graft until it has grown together with the bone. [44-46] The most frequently used fixation devices are shown in Figure 12 [9]. Adjustable loop devices (Figure 12 A) have the advantage of preserving bone structure as described in the following chapter. Furthermore, they allow a re-tensioning of the graft and the surface of the graft, which is in contact with the bone, is maximized [46]. However, they may have the

disadvantage of loop lengthening after the insertion, which could lead to clinical failure [9, 10, 46]. On the other hand, fixed loop device (Figure 12 B) do not have the disadvantage of possible lengthening. Moreover, in previous studies the fixed loop devices, such as EndoButton (Smith & Nephew, Massachusetts), showed good results considering the graft slippage. However, there were clinical difficulties reported as the loop length is fixed and the tunnel has to be drilled to a specific loop-length. Any measurement error could lead to clinical failure. [47-49] Another standard fixation device is the cross pin (Figure 12 C), which has shown good results regarding the strength of the fixation. However, intraoperative complications have been reported [50, 51]. The fourth commonly used fixation device is the interference screw (Figure 12 D). However, for this fixation device, it has been reported, that the graft slips during daily activity, which is a major disadvantage. Furthermore, the surface area between graft and bone is larger when using cross pins as opposed to interference screws. [52-54]

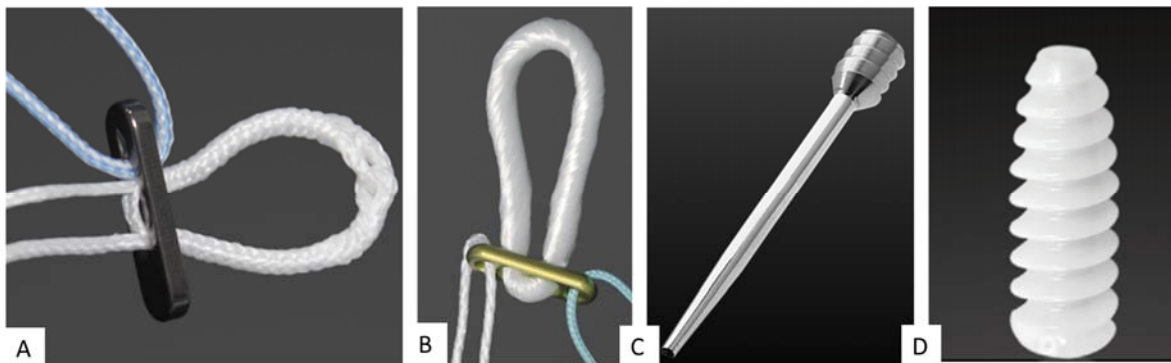


Figure 12: Most frequently used fixation devices: Adjustable loop device (A), fixed loop device (B), cross pin (C), and interference screw (D) The images shown in C & D have been modified from refs. [55, 56].

1.5. Application of an Adjustable Loop Device

Since this work focuses on an evaluation of different ALDs this type of fixation is described in more detail here. Figure 13 shows a prepared hamstring autograft with an ALD (TightRope, Arthrex, Naples, USA). After extracting the graft, it is prepared by folding it and threading it through the loops of the adjustable loop devices and sewing the two ends together.

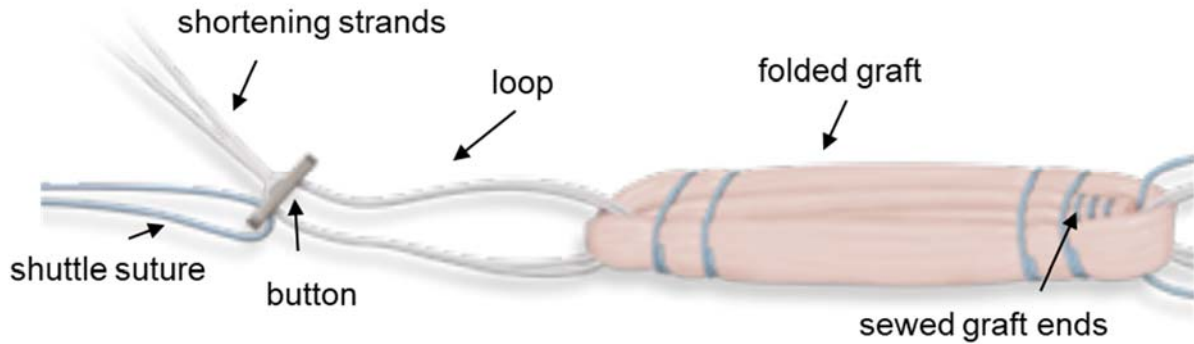


Figure 13: Hamstring autograft with ALD (TightRope, Arthrex, Naples, USA). This figure has been modified from ref. [57].

For the preparation of the bones, a tunnel is arthroscopically drilled into the femur and the tibia. Additionally, two sockets are created as represented in Figure 14 A, in order to provide room for the graft. The diameter and the length of the graft are measured before the tunnels and sockets are created. In an ideal case the graft has a length of 70 mm. In that case, the socket in the femur is drilled 20 mm deep (Figure 14 B, indicated in blue) and the one in the tibia 30 mm deep (Figure 14 B, indicated in red). The distance between the distant ends of the femoral and tibial sockets should be at least 10 mm longer than the inserted graft to ensure that the graft can be fully tensioned. If the maximum of intra-articular length is 30 mm as represented in Figure 14 B (green), there will be approximately 20 mm of graft in the femoral (blue) and tibial (red) socket. Drilling the tunnel with a smaller diameter than the socket has the advantage that it preserves bone for cortical fixation. [58]

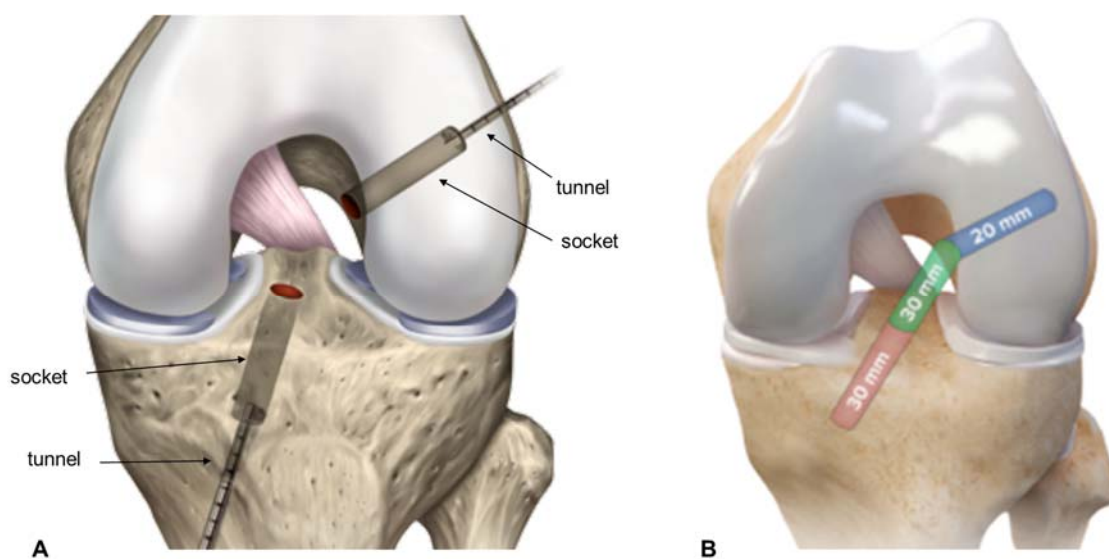


Figure 14: (A) shows the tunnels and sockets drilled into femur and tibia while (B) displays the socket and the intra-articular length. The figure has been modified from ref. [58].

Figure 15 displays the insertion and fixation of the graft in two steps. First, the ALD is passed through the femoral socket and the subsequent tunnel (Figure 15 A). The shortening strands are pulled laterally in line with the graft in order to introduce it fully into the socket. After femoral fixation, the ALD is passed through the tibial socket and subsequent tunnel and the shortening sutures are pulled (Figure 15 B). [59]

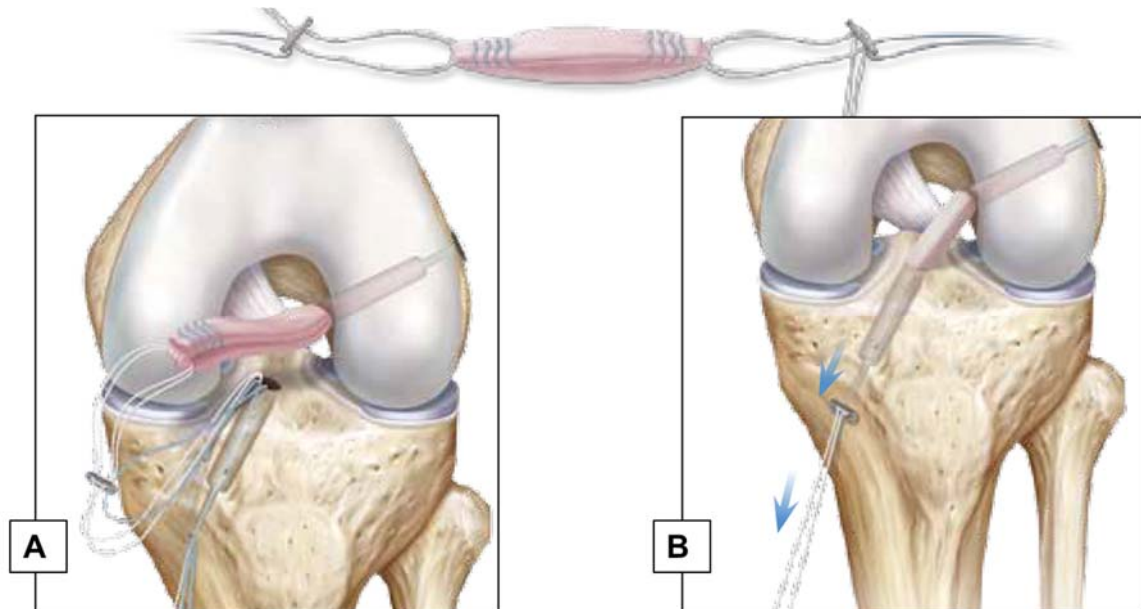


Figure 15: ACL reconstruction using an ALD for the graft fixation; Panel A shows the graft passed through the femur while panel B shows the insertion of the graft into the tibia. The figure has been modified from ref.[59].

1.6. Analysis of the Development Process of a Medical Device

The medical device *TightRope II*, which is a central aspect of this thesis, is not on the market yet. Therefore, the analysis of the development process is essential. The development of a medical device from the idea to the application on the patient includes 5 phases that are illustrated in Figure 16.

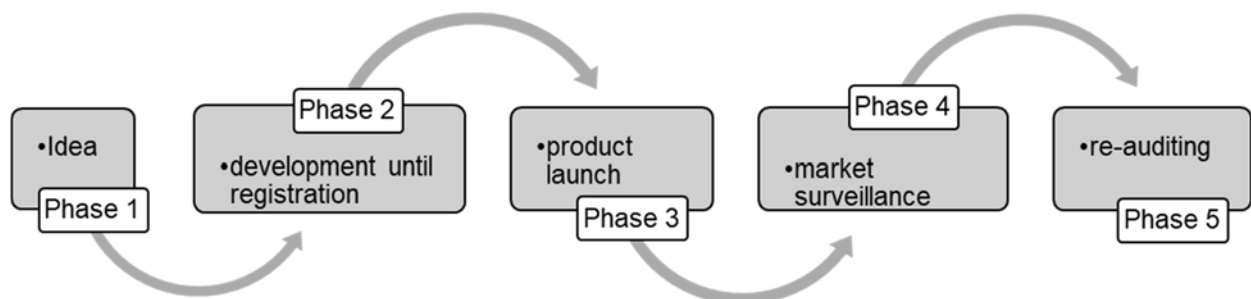


Figure 16: Five phases of the way to the market of a medical device [60].

In phase 1 someone, generally a doctor, a technician, or an engineer has an idea to invent a medical device for the treatment of a disease or to improve an already existing device. The second phase comprises the whole development process until the registration on the market. The “specification sheet” is fundamental for every development process; it contains the analysis and grading of the risk factors. Furthermore, all national and international normative and legal requirements of the new product are included in the specification sheet. [60]

The requirements for medical devices are defined in several national laws and regulations. In May 2017, a new European regulation, the medical device regulation (MDR) has been implemented. It replaces the directive 90/385/EEC for active implantable medical devices (AIMD) and the directive 93/42/EEC for other medical devices (MDD). The regulation of in vitro diagnostics stays separated, since the directive 98/79/EG for in vitro diagnostics is replaced by the in vitro diagnostic regulation (IVDR) (see Figure 17). As a European regulation, the MDR has to be followed directly and does not need to be transposed into national law such as directives. The MDR is valid since May 25th, 2017, however there is a transition period of three years until May 26th, 2020. Within this period, devices can be certified in accordance with the MDR or the directives and national laws mentioned above. For devices certified before May 25th, 2017 the certificate remains valid until the date indicated on the certificate. An exception is made for certificates, which are issued in accordance with annex 4 of directive 90/385/EEC or annex IV of directive 93/42/EEC; those become void not later than on May 27th, 2022. Certificates that are issued in accordance with the directives and national laws, within the transition period are valid until the date indicated on the certificate. However, they become invalid on May 27th, 2024 at the latest. [61, 62]

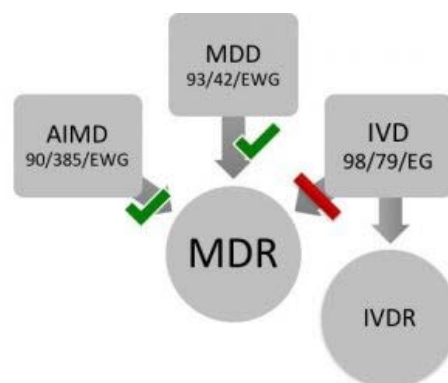


Figure 17: Schematic of changes in directives and regulations: AIMD & MDD are replaced by MDR, IVD is replaced by IVDR [61].

As mentioned above, the specification sheet does not only include legal requirements but also risk factors, which are usually covered in a risk management process. The risk factors have to be kept minimal and any remaining restrictive risk has to be smaller than the clinical benefit. The risk factors influence the classification of a medical device into one of the following four classes: I, IIa, IIb or III. With an increasing risk the class, to which the device is assigned, rises. In addition to the potential risk, the type and duration of an application are further aspects, which affect the classification. In order to ensure a good process and product quality a quality management system (QMS) has to be implemented. [60] The demands for the QMS are specified in the following two standards, EN ISO 13485:2016 (medical devices - quality management systems - requirements for regulatory purposes) and EN ISO 14971:2013 (medical devices - application of risk management to medical devices). Quality management systems, that are certified according to EN ISO 13485:2016 meet the European legal requirements, while the quality management systems that are certified according to both above mentioned standards fulfill a major part of the international requirements. [63, 64]

Another essential part of the development process is the conformity assessment. The conformity assessment according to the MDR shall provide evidence that the medical device meets the safety and performance requirements of annex I. In contrast the conformity assessment according to the MDD 93/42/EWG only provides the evidence that the basic requirements of annex I are met. Depending on the class of the medical device there are different options for the conformity assessment. [61] The options for an adjustable loop device according to the MDR are described in chapter 4.1.2.

The market launch of the new device takes place in phase 3. One major aspect within the market launch is the training of the users, since the success of the treatment depends on the correct application. Once the product is on the market, phase 4, which includes the monitoring of the product on the market, starts. During the final phase, re-audits are performed. The quality management system has to be re-certificated every three years, while a medical device needs a product-recertification at least every 5 years. [60]

2. Aim of this Thesis

The selection of a graft fixation device is an important factor that determines the outcome of an anterior cruciate ligament reconstruction. Before the healing process is completed, the graft is dependent on tibial and femoral fixation devices to maintain normal ACL graft tension. Among various devices, the use of an adjustable loop suspensory fixation device in soft-tissue graft reconstruction attracts current interest. An advantage of the ALD is the ability to draw the graft to the depth of the bone tunnel to achieve adequate graft tension while minimizing the empty space in the tunnel. However, an increase in the length of the graft-fixation device construct during the early postoperative period can lead to micromotion at the graft-bone interface, loss of graft tension, and clinical failure. Recent biomechanical studies have discussed possible elongation of the ALD under cyclic physiologically relevant loading condition.

Since previous studies discovered disadvantages of the adjustable loop device (*TightRope*) from Arthrex Inc. (Naples, USA) compared to competitor devices, Arthrex has developed an improved version the so-called *TightRope II*. Therefore, the evaluation of the development process of *TightRope II* including the classification according to the MDR and the investigation of possible ways for the conformity assessment are part of this study. A further aim of this study is to perform a comprehensive controlled laboratory investigation to examine the biomechanical properties of commonly used cortical fixation devices including *TightRope II*.

3. Materials and Methods

This chapter is divided into three parts; The analysis of the development process of *TightRope II* (Arthrex, FL, USA), the comparison of different ALD designs on the market, and biomechanical tests of the ALDs. The adjustable loop devices used in the comparison also represent the seven test groups for the biomechanical tests, with eight samples each. Additionally, two groups of fixed loop devices were included into the tests as reference groups. Due to a lack of availability, the group of *EndoButton* (Smith & Nephew, London, Great Britain) consisted of only five samples in the first test series. Of the ALD *TightRope II* a *polished* and a *non-polished* version was tested. Figure 18 shows the devices, which were used for the biomechanical test series. The FLDs are presented in Figure 18 A and B, while Figure 18 C-H shows the ALDs. The *non-polished* version of the *TightRope II* (Arthrex, USA) is not shown, since the difference to the *polished* version would not be recognizable in this picture.

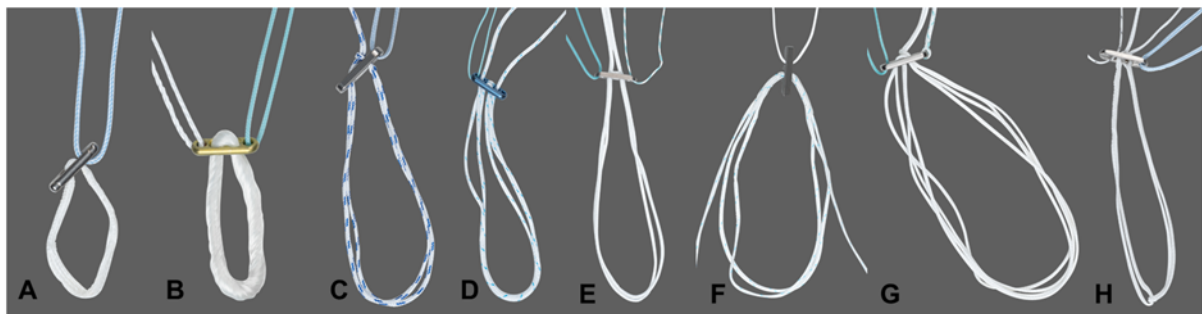


Figure 18: The nine different groups of cortical fixation devices are presented. (A) *RetroButton* (Arthrex, USA), (B) *EndoButton* (Smith and Nephew, Great Britain), (C) *GraftMax* (ConMed Linvatec Inc., USA), (D) *UltraButton* (Smith and Nephew, London, Great Britain), (E) *ProCinch* (Stryker, USA), (F) *ToggleLoc* (Biomet, USA), (G) *RigidLoop* (Mitek Sports Medicine, DePuy Synthes, Switzerland), (H) *TightRope II* (Arthrex, Florida).

3.1. Development Process of *TightRope II*

The development process of *TightRope II* at Arthrex was investigated by interviewing an expert. In several subsequent discussions the four phases of the development process were analyzed. The decision whether to use the *polished* or *non-polished* version of *TightRope II* (Arthrex, USA) was identified as a key part of the development process. Therefore, both versions were included in the first two biomechanical test

series, the ALD loop shortening and ALD stability single device test, in order to discover possible differences.

Another important factor within the development process of a new medical device is the classification. *TightRope II* was classified according to the rules of the new medical device regulation. Therefore, the 22 rules of the regulation have been analyzed in order to determine, which rule applies. Additionally, the conformity assessment for a new medical device is of paramount importance. The medical device regulation was investigated in detail in order to discover the different possibilities for the new device.

3.2. Evaluation of Different ALD Designs

In order to determine the design variations, the adjustable loop devices were carefully examined by a detailed inspection of the buttons and sutures. Furthermore, the instruction manuals, the surgical instructions, and the brochures of the devices were studied. Special focus was placed on the operating and locking mechanism. The number of strands and the transmission ratio were specified as relevant parameters. The different designs had an influence on the test set up of the loop-shortening test. The settings of the loop shortening test were different depending on the number of strands and the corresponding transmission ratio. Another important issue was the operating mechanism, as it had an impact on the way the device was inserted into the set up. Furthermore, the locking mechanisms were analyzed as differences in the results according to the different locking mechanism were expected. Table 2 displays the most important design parameters of the investigated ALDs.

Table 2: Overview over the design details of the analyzed ALDs, CFT (chinese finger trap). [65-70].

	material	transmission ratio (i)	operating mechanism	locking mechanism	number of strands	CE sign
<i>BIOMET ToggleLoc</i>	<u>Strands:</u> UHMWP <u>E</u> <u>Button:</u> titanium	2:1	single-handed (antegrade)	CFT	4	CE 0086
<i>ConMed GraftMax</i>		2:1	single-handed (retrograde)	button lock	4	CE 0086
<i>Smith & Nephew Ultrabutton</i>		3:1	single-handed (retrograde)	CFT & two loops running over button	6	CE 0086
<i>Stryker ProCinch</i>		2:1	alternating (retrograde)	CFT	4	CE 0197
<i>DePuy Synthes Rigidloop</i>		4:1	single-handed (retrograde)	button lock & two loops running over button	8	CE 0086
<i>Arthrex TightRope II polished & non-polished</i>		4:1	alternating (retrograde)	CFT & button lock	4	not yet

3.2.1. Transmission Ratio

The transmission ratios vary depending on the number of strands and on how the suture is guided through the button. Every suture loop is counted as two strands. For example, *TightRope II* (Arthrex, USA) and *ProCinch* (Stryker, USA) both have four strands. However, they do not have the same transmission ratio. The reason for that is the difference in the guidance of the suture. As shown in Figure 19 A, *TightRope II* has two interconnected loops. Therefore, the transmission ratio of *TightRope II* (Arthrex, USA) is higher than the one of *ProCinch* (Stryker, USA) shown in Figure 19 B. Depending on the transmission ratio, the values for the loop shortening were altered in the test settings (see chapter 3.3.1).

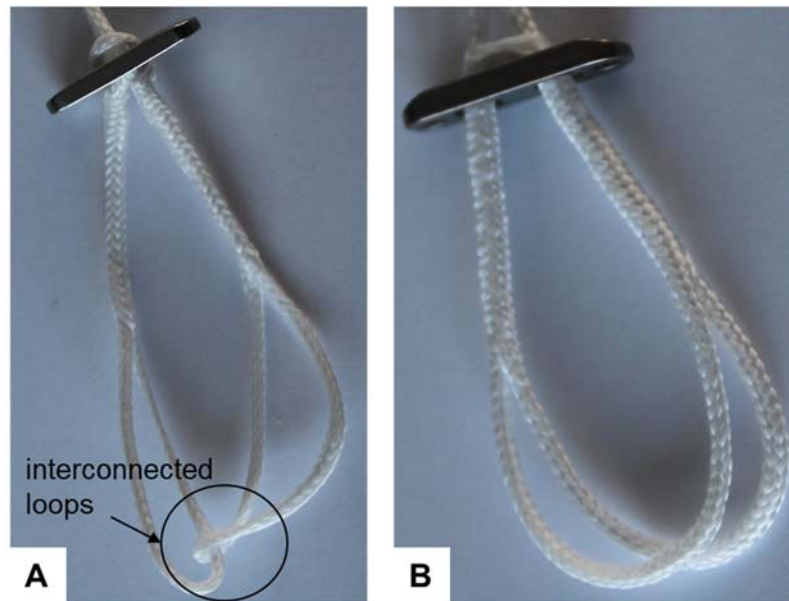


Figure 19: Pictures of TightRope II (Arthrex, USA) (A) with marked interconnected loops and ProCinch (Stryker, USA) (B). Both devices have four strands.

3.2.2. Operating Mechanism

The operating mechanism of each ALD describes the procedure to shorten the loops. Within this evaluation the following two mechanisms were identified: alternating and single-handed. Single-handed means that the loop can be shortened by only pulling one strand, while alternating means that the loop is shortened by pulling the two shortening strands in turns until the loop has the required loop length. For example the shortening sutures of the ALD *ProCinch* (Stryker, USA) have to be pulled alternating until the eyes in the shortening strands are at the same height (see Figure 20 A), while the ALD *Rigidloop* (Mitek Sports Medicine, DePuy Synthes, Switzerland) has to be operated single-handedly (see Figure 20 B). Another influencing factor is the direction in which the shortening strands are pulled. Hereby ALDs where the shortening strands are pulled away from the loop are called retrograde (see Figure 20 A & B) and ALDs where the shortening strand is pulled in the direction of the loop are called antegrade (see Figure 20 C). Depending on the operating mechanism specified by the manufacturer the test settings of the loop shortening test were adapted.

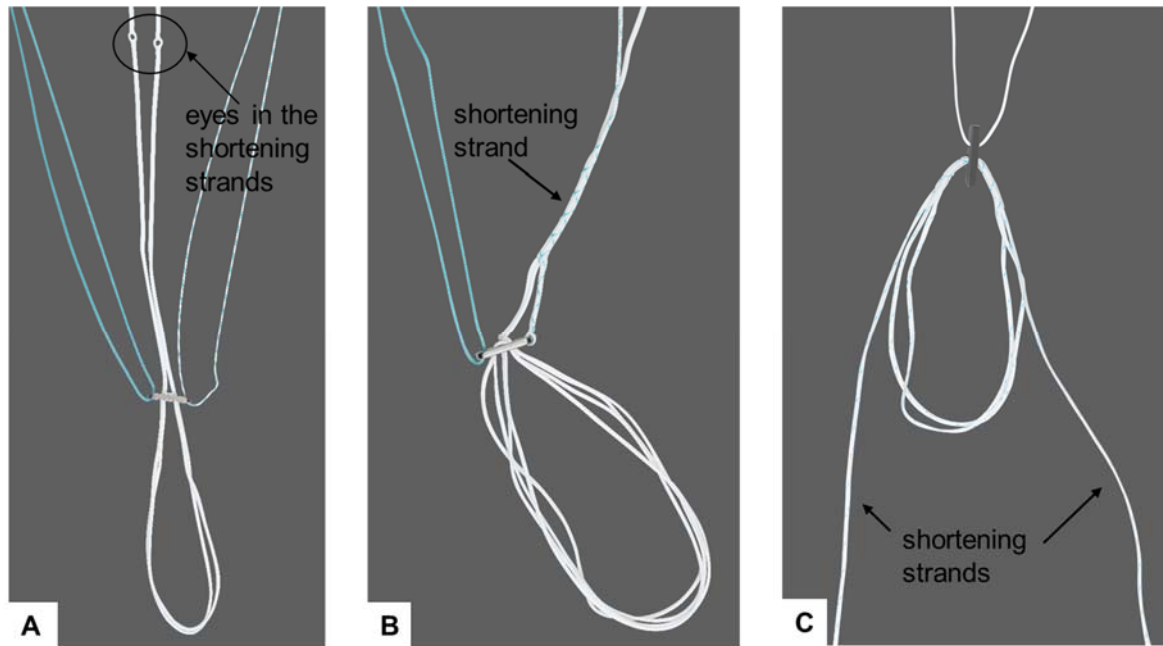


Figure 20: (A) Picture of the ALD ProCinch from Stryker with its two shortening strands, which need to be pulled alternating. (B) Picture of the ALD Rigidloop from DePuy Synthes, which has to be operated single-handedly. (C) Picture of the ALD ToggleLoc, with the antegrade shortening mechanism.

3.2.3. Locking Mechanism

Among the different ALDs two locking mechanism were identified, the button lock and the so-called chinese finger trap (CFT).

Figure 21 A displays the ALD *GraftMax* (ConMed Linvatec Inc., USA), which has a button lock. As shown in Figure 21 B the loop (red) is running over the shortening strands. When the loop is loaded the shortening strands are clamped between the button and the loop.

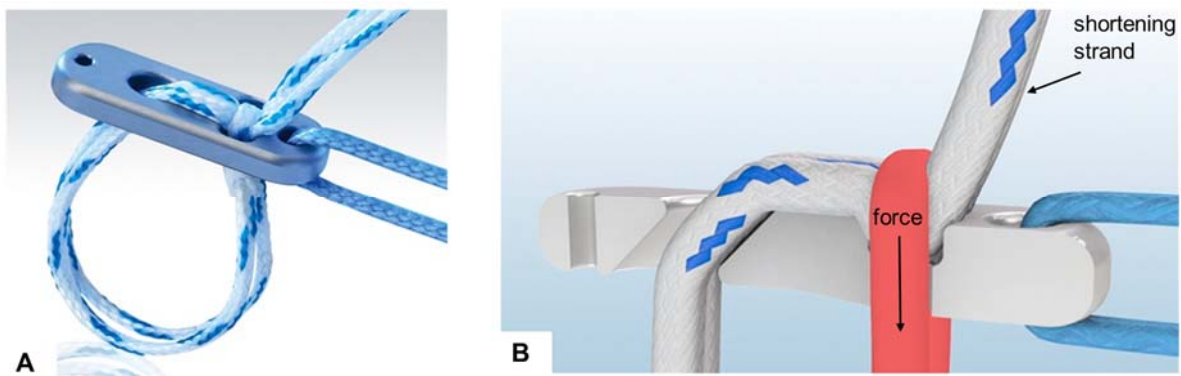


Figure 21: Pictures of the ALD *GraftMax* [71] and a medial cut of the button (B), this figure has been adapted from ref. [72].

The second locking mechanism is suture based and relies on a chinese finger trap, hereby one suture is running through the other. Figure 22 shows the ALD *ProCinch* (Stryker, USA), which is based on the CFT as locking mechanism. The blue arrow marks the position where the blue marked suture runs into the red marked one and vice versa. As displayed in Panel B the diameter of the suture decreases when both ends are tensioned. Therefore, the outer suture entraps the inner one when tension is applied to both ends.

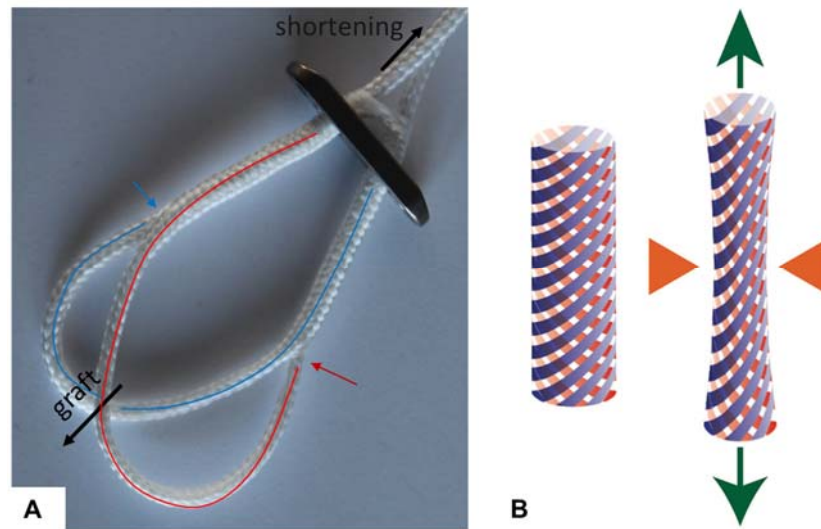


Figure 22: Picture of the ALD *ProCinch* (Stryker, USA) with its locking mechanism indicated (A) and schematic drawing of the function of the locking mechanism (B).

3.3. Test Methods and Setup

3.3.1. ALD Loop Shortening Test

This test series was performed to evaluate and compare the loop shortening behavior of the ALDs. The loop shortening behavior includes two different aspects, the accuracy of the shortening mechanism and the settling effects of the loops.

A biomechanical testing machine, with a dynamic load cell and a suture clamp was used to carry out this series of tests. Furthermore, an optical measurement system, which can detect 3D movements, was connected to the biomechanical testing machine. Table 3 lists the components used for the tensioning test. The devices presented in Figure 18 were tested. Before the loop shortening test was started, every device was loaded with eight kilograms for five minutes to reduce initial settling effects.

As preparation for the tests, the loops were adjusted to a loop length of 65 mm, to ensure consistent testing conditions. The test settings were configured for every ALD depending on the transmission ratio and the operating mechanism.

Table 3: List of the components used for the loop shortening tests are listed in this table.

components	article number	description
<i>Instron ElectroPuls E3000</i>	302583	<i>biomechanical testing machine, force measurement accuracy $\pm 0.5\%$ of the displayed value or 0.005% of the nominal force of the load cell</i>
<i>dynamic load cell</i>	141235	<i>dynamic rating ± 5 kN</i>
<i>hydraulic clamp</i>	17268N106U	<i>suture clamp with pneumatic foot switch</i>
<i>Aramis GOM</i>	15013FB	<i>optical measurement system</i>
<i>Titanar B 75 objective</i>	7520178	<i>35mm objective (Pontos 4M) (2358 x 1728 pixel)</i>
<i>weight hanger</i>	AR-1607	<i>1.5 kg weight</i>
<i>weights</i>	AR-1608G	<i>11x 1 kg weight</i>
<i>weights</i>	AR-1609G	<i>8x 0.5 kg weight</i>
<i>disc</i>	-	<i>slotted disc</i>
<i>table</i>	-	<i>testing table to position the slotted disc</i>

The test setup included a slotted disc, where the buttons were placed, and the loops could be threaded through (Figure 23). The shortening strand was trapped in the suture clamp of the testing machine and the hook was mounted into the loop. Five marker-dots were placed on the hook to detect its 3D position by the optical measurement system. Any change in position of the hook could thereby be detected with the camera. Every sample was tested at six load-levels, regarding the load applied to the loop via the hook (see Table 4).

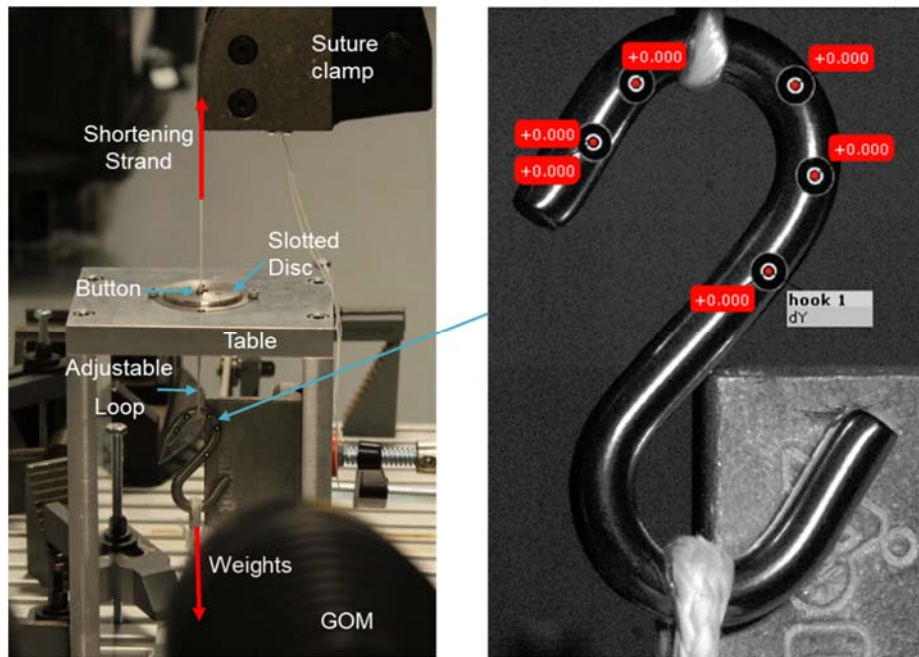


Figure 23: Picture of the test setup used for tensioning test.

All tests were executed according to the following protocol (see Figure 24):

- **1st step:** The loop was loaded via the hook with the weight for the corresponding load level. The shortening strand of the ALD was preconditioned, which means that the machine actuator with the attached suture clamp pre-stretched the suture by moving up until the preconditioning force was reached. The preconditioning forces were defined as one-third of the applied weight of the six load levels (see Table 4). After the preconditioning the first picture (G1) of the hook was taken to obtain the reference position.

Table 4: Weights applied to the loop and the according forces used for the preconditioning.

applied weight in kg	preconditioning force in kg
1.5	0.5
3.5	1.16
5.5	1.83
7.5	2.5
9.5	3.16
15	5.0

- **2nd step:** The loop was shortened by 10 mm due to the upwards movement of the test machine actuator with the attached suture clamp. Then, the second picture

(G2) was taken, to analyze the loop length after shortening. The distance d , which the suture clamp had to move up, to reach a loop shortening of 10 mm was calculated through a multiplication with the respective transmission ratio i of the ALDs.

$$d [mm] = i * 10 [mm] \quad (1)$$

- **3rd step:** The shortening strand was unloaded by the backwards movement of the test machine actuator to its initial position and the third picture (G3) was taken. After unloading the shortening strand, the locking mechanism is responsible to keep the loop at the shortened length.
- **4th step:** The load of the hook was changed to the maximum load (15 kg) and the last picture (G4) was taken. This step was included in order to record the settling effects of the ALDs when higher load is applied.

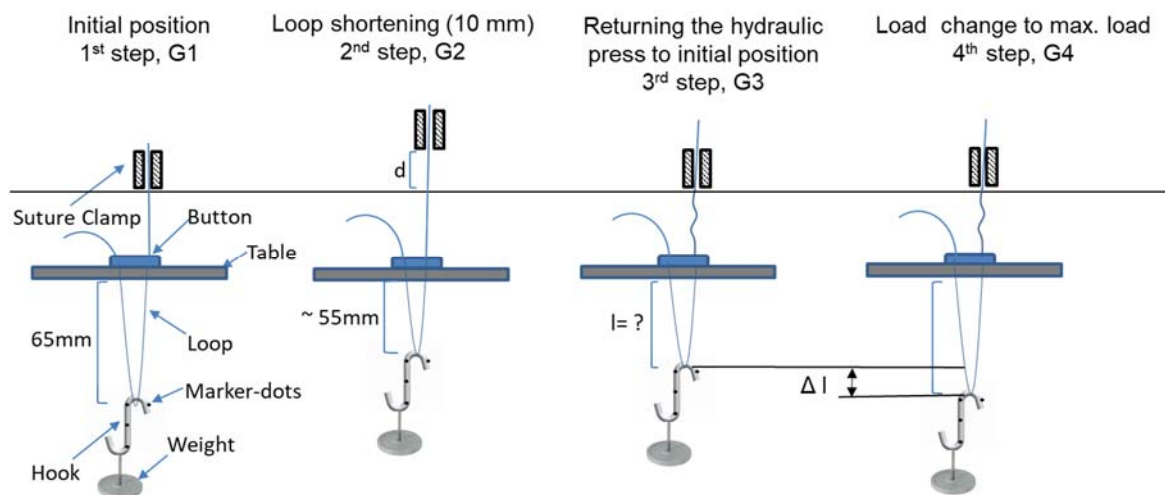


Figure 24: Schematic representation of the loop shortening test process.

3.3.2. ALD Stability Test

To evaluate the irreversible elongation of the adjustable loop devices under cyclic loading, stability tests were performed in two different test series. First, a single device test was executed, to test the isolated mechanical properties of the ALDs. In continuation, the ALDs were tested in combination with a tendon to investigate the behavior of the ALDs in an environment that is closer to that of the clinical application. The devices presented in Figure 18 were tested. For both series, a biomechanical dynamic testing machine with a 2 kN load cell was used. Table 5 presents the components used for this test series. In both series the devices were tested for 3000 cycles of loading and complete unloading with increasing load levels between 50 and 300 N. These testing conditions were chosen because *Monaco et al.* [73] reported that repetitive loading and complete unloading situations are the most adequate conditions to evaluate the stability of ALDs. The maximum load level of 300 N were chosen according to previously performed studies [9, 45, 46, 74].

Table 5: Overview over the components used for the stability test.

components	article number	description
<i>Instron ElectroPuls E10000</i>	141235	<i>biomechanical testing machine, force measurement accuracy $\pm 0.5\%$ of the displayed value or 0.005 % of the nominal force of the load cell</i>
<i>dynamic load cell</i>	302583	<i>dynamic rating +/- 2 kN</i>
<i>bovine tendon</i>	-	<i>diameter: 8 mm length: 15 mm</i>
<i>weight hanger</i>	AR-1607	<i>1x 1.5 kg</i>
<i>weights</i>	AR-1608G	<i>5x 1 kg</i>
<i>graft sizing block</i>	AR-1886	<i>4.5-12 mm holes in 0.5 mm increments</i>
<i>FiberLoop</i>	AE 7234	<i>#2 with straight needle</i>
<i>GraftPro Base</i>	AR-2950D	<i>station for graft preparation</i>
<i>marker pen</i>	AR 1897P	<i>skin marking pen</i>
<i>scalpel 11</i>	BM-428-010	<i>surgical scalpel</i>
<i>scalpel 20</i>	BM-428-012	<i>surgical scalpel</i>

3.3.2.1. Single Device Test

The test setup for the single device test is displayed in Figure 25 A, showing the tested device in black. The ALDs and FLDs were fixed in the setup between two metallic components to apply loads on the device. The cortical button and suture loop were fixed onto a slotted disc (brown) attached to the test machine actuator. A pin (green) on the baseplate of the machine secured the suture loop. Before the ALD was mounted into the test setup, the loop length was adjusted to 25 mm, to ensure equal conditions for each test. This test setup represents worst case conditions, since the forces are transmitted with very little friction loss at the metallic pin. To simulate an intra-articular environment the tests were performed in water, as shown in the picture of the setup (Figure 25 B).

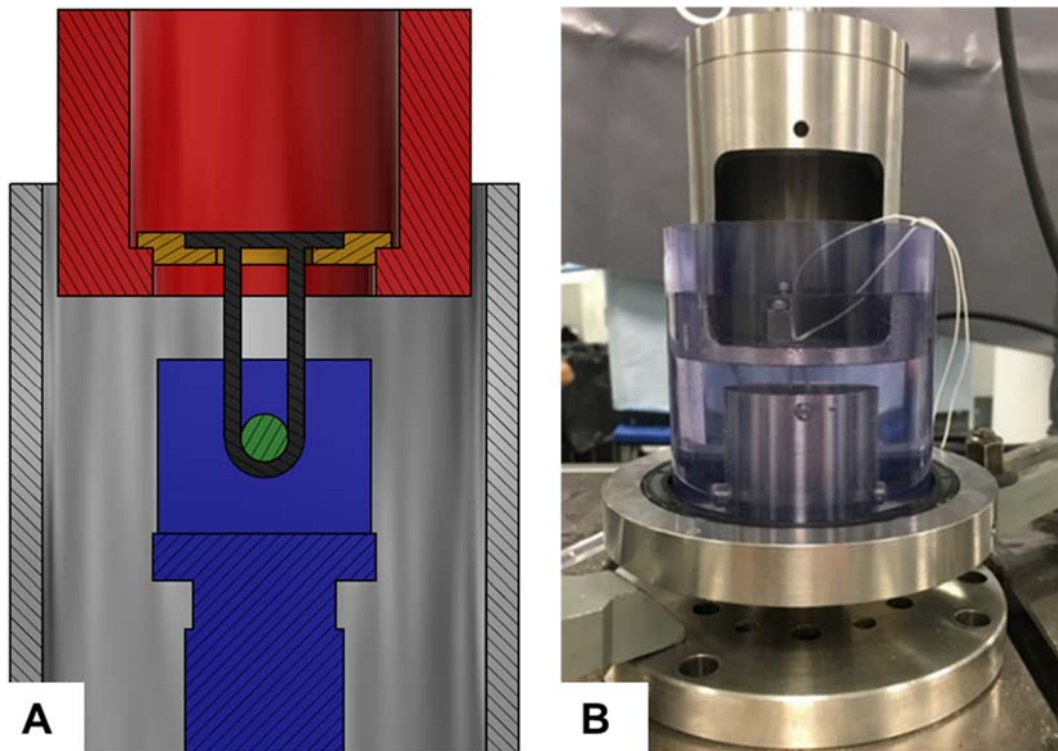


Figure 25: (A) Schematic drawing of the test setup for the stability single device test, the tested device is shown in black. (B) Picture of the test setup for the stability single device testing.

The tests were performed according to the protocol displayed in Figure 26, which includes 3000 cycles of loading and complete unloading of the loop at six different load levels. As the biomechanical testing machine requires a minimal tension, a tension of 5 N was defined as the zero point for the calibration. At the beginning of the tests, the devices were preconditioned to a load of 50 N for 5 seconds to remove slack from the loops. After that, cyclic loading was performed at a rate of 0.75 Hz. Each cycle

consisted of a loading phase, where the loop was tensioned to the defined load, by moving the machine actuator upwards and the following unloading phase, where the actuator was moved down again over a defined distance of 1.5 mm to assure complete unloading. After every 500 cycles, the load was increased by 50 N. The minimum and maximum applied load were 50 and 300 N, respectively. The test was ended after 3000 cycles were completed or if the elongation of the loop reached a threshold of 8 mm.

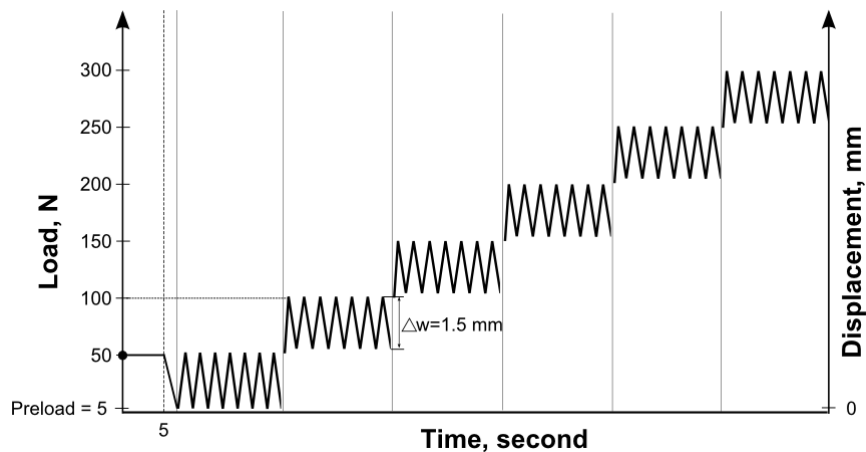


Figure 26: Testing protocol of the single device test with load and displacement on two x-axis, as functions of the time.

3.3.2.2. Device -Tendon Test

In order to evaluate the behavior of the ALDs in an environment that resembles that of the clinical application more closely, a stability test series was performed using bovine tendons as grafts. Major advantages of using animal specimens as opposed to human tendons are a better availability as well as an improved comparability of the specimen among each other. Bovine tendons are considered to have similar viscoelastic and structural properties to human tendons. [75]

In order to harvest grafts for the device tendon testing, feet from freshly slaughtered bovines were acquired from the local slaughterhouse. All bovines were roughly 3 years old and had similar physical characteristics. The soft tissue was removed until the extensor tendons were exposed (see Figure 27 A). After extracting the tendons with a length of at least 150 mm, they were frozen in order to keep them fresh until the

preparation could be continued within the next days. Freezing and thawing the tendons once does not influence their biomechanical properties [76].

During the follow-up preparation, the tendons were unfrozen and cleaned, which means that any remaining connective tissue was removed. Afterwards, the tendons were split into two parts, as indicated with the black dashed line in Figure 27 B. Furthermore, they were cut to a diameter of 8 mm when folded. The graft was pulled through the hole in the graft-sizing block, to measure the diameter (Figure 27 C). If necessary, the diameter was further reduced until the 8 mm were reached. During all preparation steps, the tendons were kept wet to prevent them from desiccating.

Directly before testing, the graft was threaded through the loop of the ALD (Figure 27 D) and the two ends were combined with 4-5 whip-stitches at the last 3 cm of the graft's ends using an *Arthrex Fiberloop* (Figure 27 E). A *FiberLoop* is a continuous loop of *FiberWire* with a freely moving straight needle. After finishing each stitching process, the needle was removed and the rest of the *Fiberloop* remained at the graft. Figure 27 F shows a finished ALD-soft tissue construct before testing.

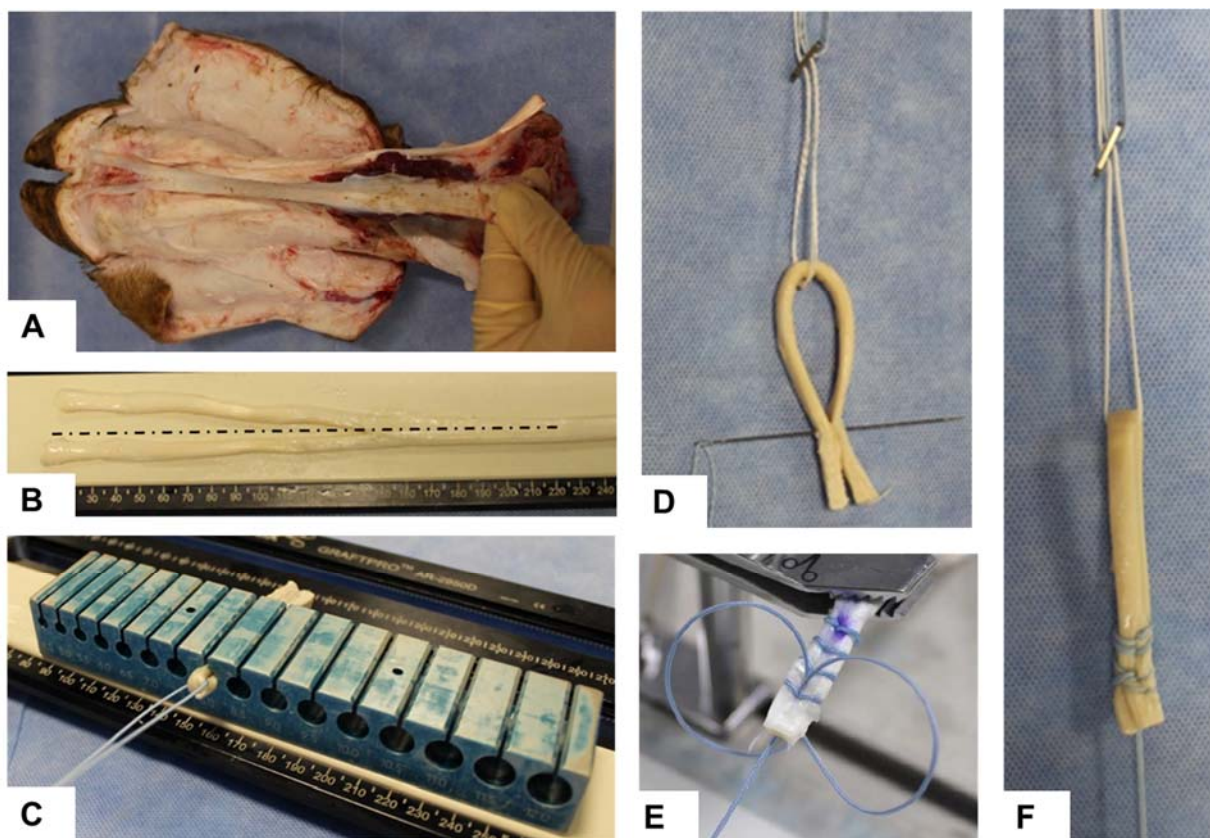


Figure 27: Pictures of the preparation steps for the bovine tendons for the stability tests. (A) Extraction of the extensor tendon. (B) Splitting the extracted tendon according to the black dashed line. (C) Pulling the folded tendon through a graft sizing block to measure the diameter. (D) Device tendon construct with initial stitch. (E) Ends of the tendon including five whip-stitches. (F) Final device-tendon construct.

After the described preparation, the device-tendon construct was mounted into the test setup as shown in Figure 28 A. The button was placed onto a slotted disc attached to the test machine actuator, in the same way as described in the single device test. In the next step, the graft was loaded with a weight of 1.5 kg, which was attached through the created loop of the *FiberLoop* (see Figure 28 B). Afterwards, the graft was marked at a length of 35 mm and the loop length of the ALD was adjusted to 25 mm for all tests. The weight was then changed to 5 kg and the graft was entrapped with a screw clamp, directly under the marked position (see Figure 28 C). Finally, the weight was removed, and the test was started.

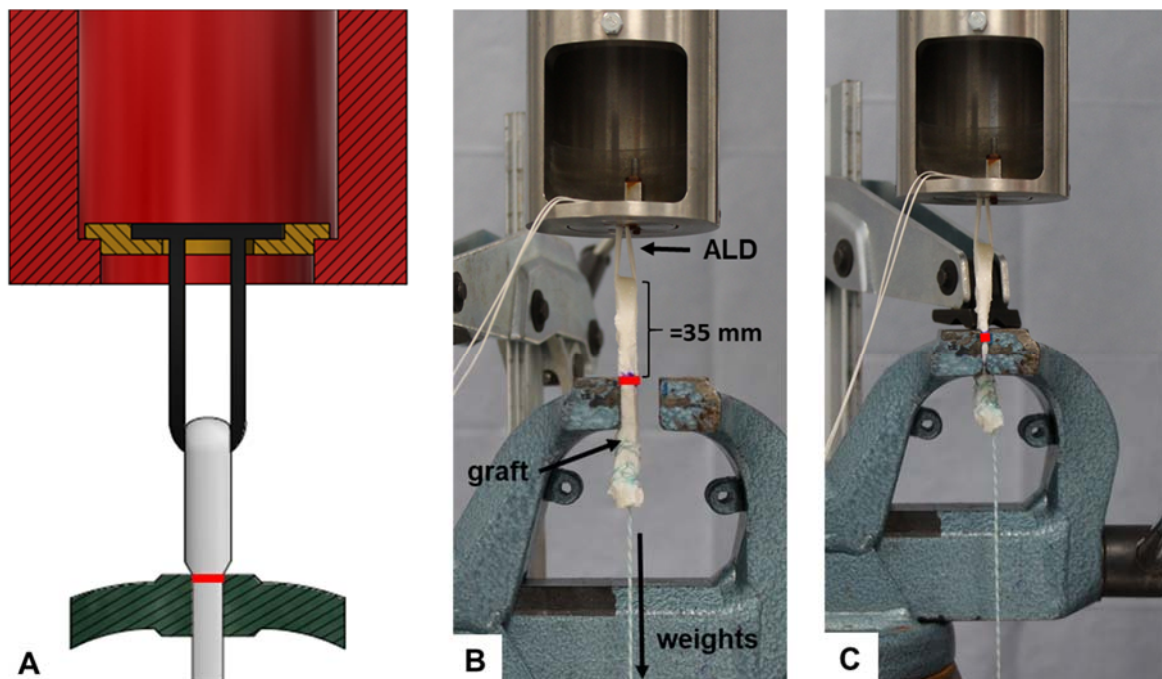


Figure 28: (A) Schematic drawing of the stability test setup. (B) Pictures of the setup preparation for the device tendon test and picture of the final test (C).

As in the single device test, the samples were tested during 3000 cycles of loading and complete unloading. The testing protocol was roughly the same as for the single device test, with the only difference being the adaptation of the value for the unloading distance Δw . The value was doubled to assure a complete unloading keeping in mind the flexibility of the tendon.

3.4. Data Analysis

3.4.1. ALD Loop Shortening Test

After completing the test series, the data sets of the optical measurement system and those from the biomechanical testing machine were evaluated using the following three programs: GOM Correlate Professional (GOM GMBH, Braunschweig, Deutschland, 2017), Microsoft Excel (Microsoft Corporation, Redmond, USA, 2016) and Matlab (Mathworks Inc., Natick, USA, 2017). To evaluate, whether there is a statistically significant difference between the tested groups the results were analyzed using SigmaPlot Statistics (Systat Software Inc, San Jose, USA, V13.0). The test results were statistically analyzed with a one-way analysis of variance (ANOVA), wherein a probability value of $P \leq 0.05$ was defined as statistically significant. The normal distribution was observed and a *post hoc Tukey* test was performed to realize an all pairwise multiple comparison.

The final force applied to the loops (F_z) was calculated by multiplying the weights mounted to the loops (m_L) with the gravitation (g) of 9.81 m/s^2 , as shown in equation 2.

$$F_z [N] = m_L [kg] * g \left[\frac{m}{s^2} \right] \quad (2)$$

To quantify the settling effects of the ALDs, a total bounce back (tbb) was defined as the value of the setting effects of the ALDs (see Figure 29). It is calculated as the difference of the vertical position of the hook between picture G4 and picture G2:

$$tbb [mm] = G4 [mm] - G2 [mm] \quad (3)$$

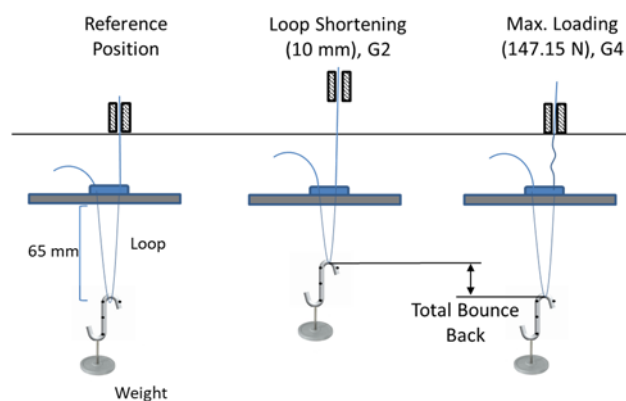


Figure 29: Schematic drawing of the total bounce back.

The average values and the standard deviation of the data sets were calculated with the function “average” and “stdev.s” in Microsoft Excel (Microsoft Corporation, Redmond, USA, 2016).

Furthermore, the error of the optical measurement system had to be considered. To keep the calibration error as small as possible the camera system had to be switched on at least 25 minutes before the first test was performed [77]. The software GOM Correlate 2017 displayed a scale error of 0.002 mm and a calibration error of 0.012 pixel for all tests. In the specification sheet, the limit for the scale and calibration errors are ≤ 0.01 mm and ≤ 0.04 pixel, respectively [77]. Thus, the measured errors are well within the limits.

Figure 30 shows a representative schematic progression of the pulling force as a function of the displacement during loop shortening recorded by the biomechanical testing machine. The shortening process may be divided into three parts, which are marked with *a*, *b* and *c* in Figure 30. In part *a* the preconditioning takes place. In part *b* the machine actuator starts to move up and the force increases. However, due to initial stretching of the suture the loop is not shortened considerably, which results in relatively small displacement. In part *c* the actual loop shortening takes place. Therefore, the force values of part *a* and *b* were excluded before the average pulling force necessary to shorten the loop was calculated.

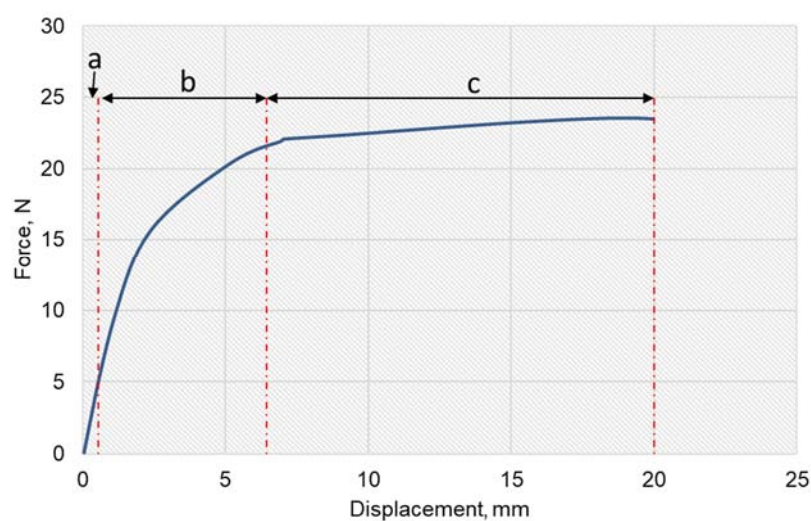


Figure 30: Schematic drawing of the force applied by the Instron to shorten the loop as function of the actual displacement of the machine actuator with attached suture clamp.

3.4.2. ALD Stability Test

The recorded data sets of both stability test series (single device test & device-tendon test) were analyzed with Microsoft Excel (Microsoft Corporation, Redmond, USA, 2016) and Matlab (Mathworks Inc., Natick, USA, 2017). Barrow et al. [9] and Ahmad et al. [10] defined an absolute displacement of 3 mm as clinical failure. Therefore, the same value was considered as failure criterion for the test samples. The absolute displacement represents the irreversible elongation of the loop when the device is unloaded.

In order to evaluate, whether there is a statistically significant difference between the ALD groups, the results were also analyzed using SigmaPlot Statistics (Systat Software Inc, San Jose, USA, V13.0). The data sets were statistically analyzed with the same methods described for the tensioning test results. The measured values of the total displacement after 3000 cycles, where statistically analyzed for those ALDs, which did not reach clinical failure. For the ALDs, that did not survive 3000 cycles, the clinical failure cycles were analyzed.

4. Results

In this chapter the development process of *TightRope II*, including the classification and the possible ways to perform the conformity assessment, are presented. Furthermore, the results of the three biomechanical test series are displayed. The data sets of the loop shortening test and the stability single device test of the *polished* and *non-polished* version of *TightRope II* are analyzed separately, in order to decide which version will be used.

4.1. Development Process *TightRope II*

The discussions lead with the expert reveals that the development process of *TightRope II* consists of four phases, which are shown in Figure 31. In order to document all relevant steps and decisions of this process, the design traceability matrix (DTM) is implemented.

In phase one, the user needs are defined by the product manager and the supporting surgeon and subsequently added to the matrix. Examples for the defined user needs are that the device should fit through a 4 mm drill hole in the bone for an ACL reconstruction and that it has to show less elongation than the previous *TightRope*. Another important part of phase one is the classification of the device. This is substantial for the following phase because the risk management builds on it.

In phase two of the process the initial design for the components is created. These designs are documented in the second part of the DTM. To assure the biocompatibility of the device, the used materials have to be defined. *TightRope II* is made out of the same materials as the already existing *TightRope*, therefore this step is simplified. Furthermore, the drawings of the components are created, and the prototypes are produced within this phase. Two versions of the *TightRope II* prototypes are produced, a *polished* and a *non-polished* button. Additionally, all testing methods have to be defined in phase two, including the pretesting methods for the two prototypes to decide which version is better. This decision is made by the engineering team, as the last step of phase two. The decision is based on the results of the pretests performed within this study.

Phase three starts with the risk analysis, where all potential risks are defined and graded according to their likelihood of occurrence and their possible consequences. Further steps of phase three are the design of the packaging as well as the first production run of the final device. The design verification is performed with the devices produced in the first production run. This is done by executing the biomechanical test series described in chapters 3.3.1 and 3.3.2. After the positive verification of the new design, the validation is performed through wet lab testing. This means that at least eight independent surgeons have to do an ACL reconstruction on a knee of a dead human donor using *TightRope II*. After the surgeries, they have to complete a questionnaire to give their feedback on the device. In the last phase of the development process, a final review of all the previously performed steps is performed, to be able to start the market launching process.

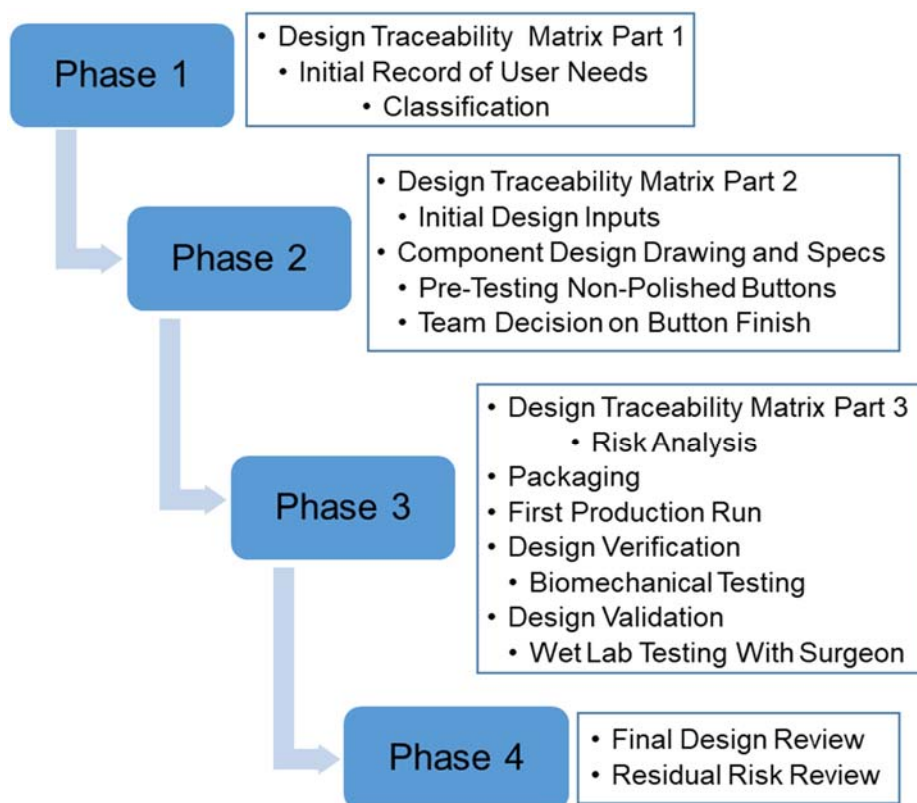


Figure 31: Illustration of the four phases and the respective main steps of the development process of *TightRope II*.

4.1.1. Classification of *TightRope II*

The new medical device regulation (MDR) of the European Union contains 22 rules for the classification of medical devices, which are presented in annex VIII, chapter III of the MDR. Those 22 rules are divided into four groups. Rule 1-4 consider invasive devices while rule 5-8 are applied for non-invasive devices. Furthermore, rule 9-13 are utilized for active devices and 14-22 are special rules. Since *TightRope II* is an invasive device, which is categorized as an ancillary component, rule 8 applies for the classification. This rule is specified as follows [62]:

“All implantable devices and long-term surgically invasive devices are classified as class IIb unless they:

- are intended to be placed in the teeth, in which case they are classified as class IIa;*
- are intended to be used in direct contact with the heart, the central circulatory system or the central nervous system, in which case they are classified as class III;*
- have a biological effect or are wholly or mainly absorbed, in which case they are classified as class III;*
- are intended to undergo chemical change in the body in which case they are classified as class III, except if the devices are placed in the teeth;*
- are intended to administer medicinal products, in which case they are classified as class III;*
- are active implantable devices or their accessories, in which cases they are classified as class III;*
- are breast implants or surgical meshes, in which cases they are classified as class III;*
- are total or partial joint replacements, in which case they are classified as class III, with the exception of ancillary components such as screws, wedges, plates and instruments; or*
- are spinal disc replacement implants or are implantable devices that come into contact with the spinal column, in which case they are*

classified as class III with the exception of components such as screws, wedges, plates and instruments.

- *are total or partial joint replacements, in which case they are classified as class III, with exception of ancillary components such as screws, wedges, plates and instruments. “*

4.1.2. Conformity Assessment

The possible options for the conformity assessment of the *TightRope II* are presented within this chapter. Article 52 of the MDR defines that a conformity assessment has to be performed for every medical device before placing it on the market. The possible conformity assessment procedures are stated in annexes IX to XI of the MDR. Since *TightRope II* is classified as a class IIb product and the options depend on the class of the device, the possible procedures for class IIb devices are presented here.

Figure 32 shows the two different ways for the conformity assessment procedure. The first option is an assessment according to annex IX, chapter I and III as well as the first part of chapter II of the MDR. It consists of an assessment of the quality management system (QMS) and the technical documentation of the device. The second option is the conformity assessment according to a combination of annex X and XI of the MDR and is carried out through a type examination and a product conformity verification. [62] Both options are explained in detail in the following subchapters.

After completing the conformity assessment successfully, the manufacturer is allowed to place the CE sign and the identification number of the notified body on the product and to issue the declaration of conformity. The CE sign confirms that the product meets the safety and performance requirements of the MDR. A medical device must not be placed on the market and put into service without a CE sign. [61]

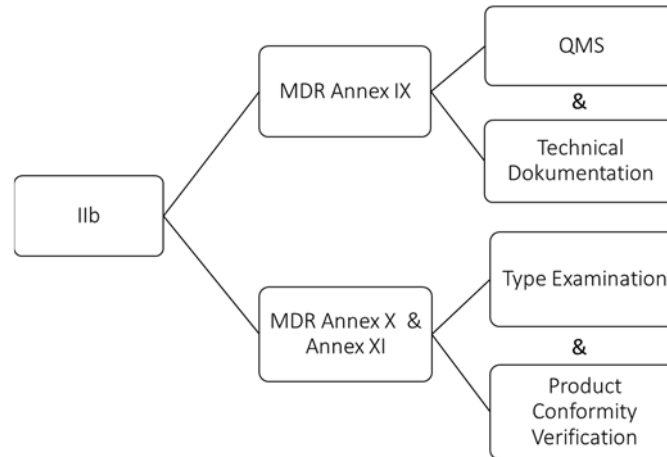


Figure 32: Flowchart of the possibilities for the conformity assessment for a class IIb medical device.

4.1.2.1. MDR Annex IX

The conformity assessment procedure, which is specified in annex IX of the MDR combines a quality management system and the assessment of the technical documentation (see Figure 33).

In order to perform the conformity assessment according to annex IX of the MDR the manufacturer is obliged to setup, document and realize a quality management system. Additionally, a quality manual that includes the aspects which the QMS is based on, has to be maintained. With the realization of the QMS the fulfillment of the regulation is ensured. Furthermore, an application for the evaluation of the QMS has to be submitted to a notified body. [62] Notified bodies are state accredited companies, mostly privately held, that are auditing manufacturers of medical devices and verify the conformity of their technical documentation with the legal requirements [61]. The application has to include all relevant documents and an adequate description of the main aspects of the QMS such as the defined quality objectives and the verification and validation procedures of the products [62].

The notified body then audits the QMS in order to verify whether all requirements are met. When the audit is completed positively, the manufacturer receives an EU-QMS certificate. To ensure that the manufacturer complies with all the specifications of the already approved QMS, there is a surveillance assessment for products of class IIb.

The manufacturer is obliged to enable the notified body to execute all necessary audits and to provide all required documents. These audits have to take place regularly at least once every twelve months. In addition to that, there are unannounced audits, which happen at randomly selected times but at least every five years. [62]

Furthermore, the manufacturer has to submit an application for the assessment of the technical documentation to a notified body. In this application the design, manufacturing process, and the performance of the device have to be specified. The notified body performs adequate physical inspections or laboratory tests or assigns the manufacturer to execute those tests. Additionally, the notified body reviews the adequacy of the clinical evidence and the clinical evaluation. After a positively completed evaluation, an EU technical documentation assessment is issued. Modifications of the approved device are possible, but they have to be accepted by the same notified body that performed the assessment of the technical documentation. [62]

In chapter III of annex IX of the MDR the administrative provisions are specified. In order to fulfill these provisions, the manufacturer is obliged to provide all essential documents to the competent authorities for a duration of at least 15 years after bringing the device on the market. Essential documents are the EU declaration of conformity, the documentation of the QMS, and any information about changes in that system, as well as decisions and reports from the notified body and the technical documentation. [62]

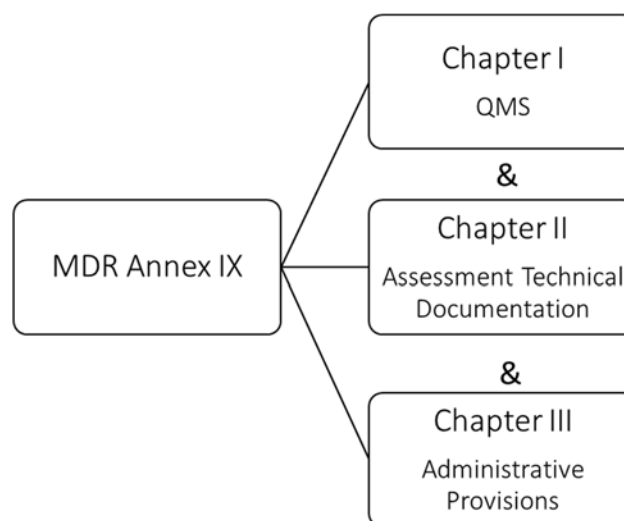


Figure 33: Flowchart of the conformity assessment procedure according to annex IX of MDR.

4.1.2.2. MDR Annex X & XI

The second option is to perform the conformity assessment based on a type examination combined with the conformity assessment based on the product conformity verification. For the product conformity verification part A (production quality assurance) or part B (product verification) of annex XI can be used (see Figure 34). [62]

The type examination is performed to ensure the compliance of the medical device with all requirements specified in annex X. To start this process, the manufacturer has to submit an application for assessment to the notified body. Furthermore, he has to confirm that the same application has not been submitted to a second notified body in parallel. Together with the application and a sample of the device (type), various documents have to be submitted, such as the technical documentation, the user manual, documentations of the risk-management process, the clinical evaluation, and the evaluation of the biocompatibility. The notified body evaluates the integrity of all documents and whether the type is produced in accordance with those documents. If all evaluations performed by the notified body are concluded positively, an EU type examination certificate is issued. Modifications of the type are possible, but they have to be approved by the same notified body that issued the EU type examination. After receiving the certificate, the manufacturer has to choose how to perform the product conformity verification, according to part A or part B of annex XI of the MDR (see Figure 34). [61, 62]

Part A describes the production quality assurance, where the manufacturer ensures the application of the QMS for his product. When this application is fulfilled, an EU declaration of conformity can be issued, which confirms that the product is conform to the type in the EU type examination certificate and all requirements of the regulations are fulfilled. [62]

Part B describes the product verification, which means that the final inspection of production is outsourced and performed by a notified body. The inspection has to be performed for every device, since the MDR does not contain batch tests, in which only parts of a group are tested. Every approved device is then labelled with the

identification number of the notified body and an EU product verification certificate is issued. [62]

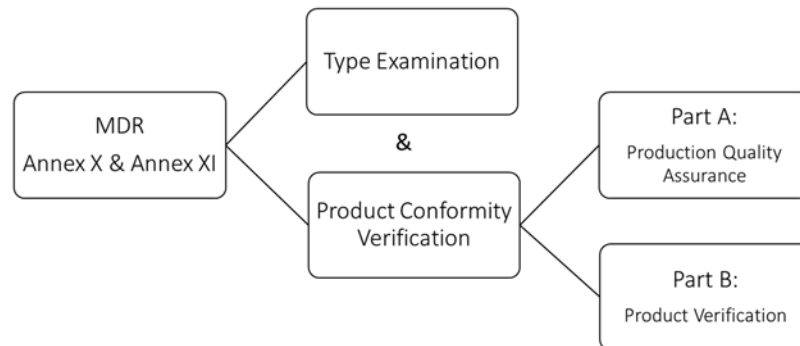


Figure 34: Flowchart of the conformity assessment procedure according to Annex X and XI of MDR.

4.2. Pre-Testing of *Polished* and *Non-Polished TightRope II* Buttons

Figure 35 shows the *non-polished* (panel A) and *polished* (panel B) version of *TightRope II*. The *non-polished* version has a rough surface while the *polished* version has a very smooth surface due to an additional processing step. The results of the loop shortening and the stability single device tests of the two versions are presented in this chapter in order to decide which version will be used further.

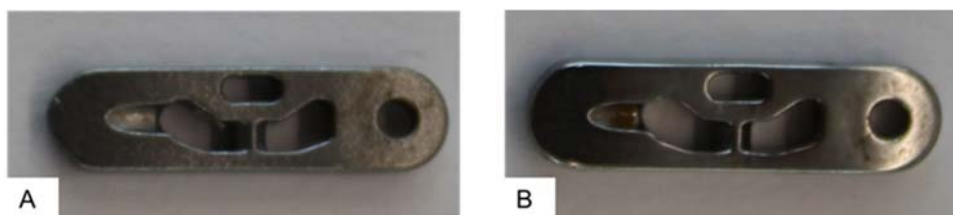


Figure 35: Picture of the non-polished (A) and polished (B) buttons of *TightRope II*.

4.2.1. Loop Shortening Test

The calculated total bounce back values of the *polished* (blue) and *non-polished* (orange) versions of *TightRope II* at the six tested load levels are shown in Figure 36. The tbb values were calculated with equation 3 as described in chapter 3.3.1.

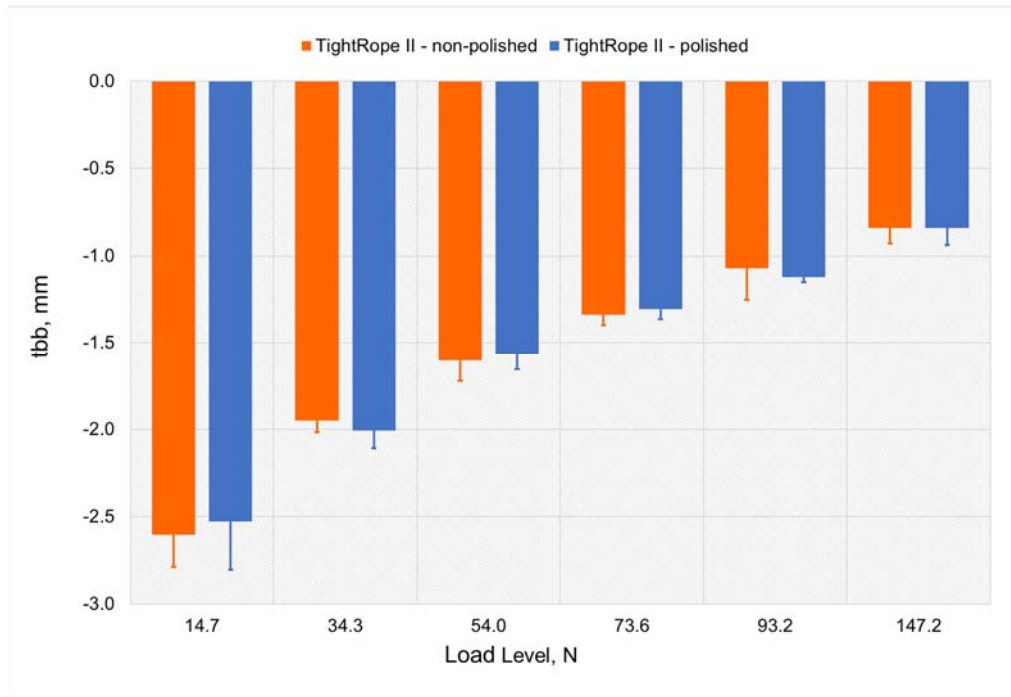


Figure 36: Average total bounce back of the non-polished and polished version of *TightRope II* (Arthrex, USA) as a function of the load level. The shown values are the average of eight measurements and the error bars represent the standard deviation between those measurements.

4.2.2. Stability Test - Single Device

As shown in Figure 37 the total displacement after 3000 cycles of loading and complete unloading of the *non-polished* version is greater than the total displacement of the *polished* version.

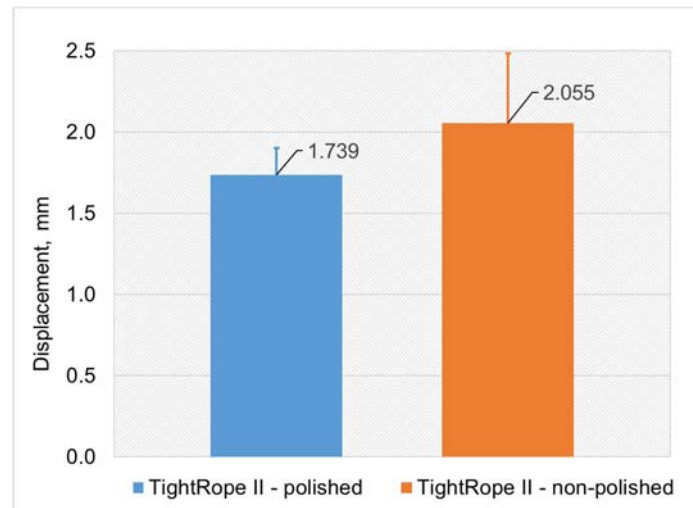


Figure 37: Total displacement of the polished and non-polished version of TightRope II after cyclic loading for 3000 cycles. The shown values are the average of eight measurements and the error bars represent the standard deviation between those measurements.

4.3. ALD Loop Shortening

The loop shortening behavior of the eight test groups is presented in this chapter. All the tests in this and the following chapters were only performed on the *polished* version of *TightRope II*. First, the analysis of the shortening accuracy is shown. Thereafter, the result of the calculated total bounce back values are illustrated. Finally, the loop shortening is displayed as a function of the tension applied by the biomechanical testing machine.

Figure 38 shows the final loop length at six different load levels for the tested adjustable loop devices after nominal shortening of 10 mm. The values shown in this figure are an average of eight measurements. The final loop length values were recorded by the optical camera system after shortening the loop, but before unloading the shortening strand of the devices. The red line, which indicates the expected position, is added as a reference and for a better comparability. The results of *RigidLoop*, *UltraButton*, and *TightRope II* show a similar shortening behavior with a shortening close to the expected

length of 10 mm. The *ProCinch* and *ToggleLoc* devices already have higher loop lengths deviations at smaller load levels with a steady increase until reaching the final load. The group of *GraftMax* shows a wide intragroup variation, which is represented by the high standard deviation, especially at the first load level. At the last three load levels the devices *GraftMax*, *ProCinch*, and *ToggleLoc* show a significantly lower shortening length than the other tested devices. The mean values and standard deviations as well as the results from the all pairwise multiple comparison of the groups are attached in appendix I.

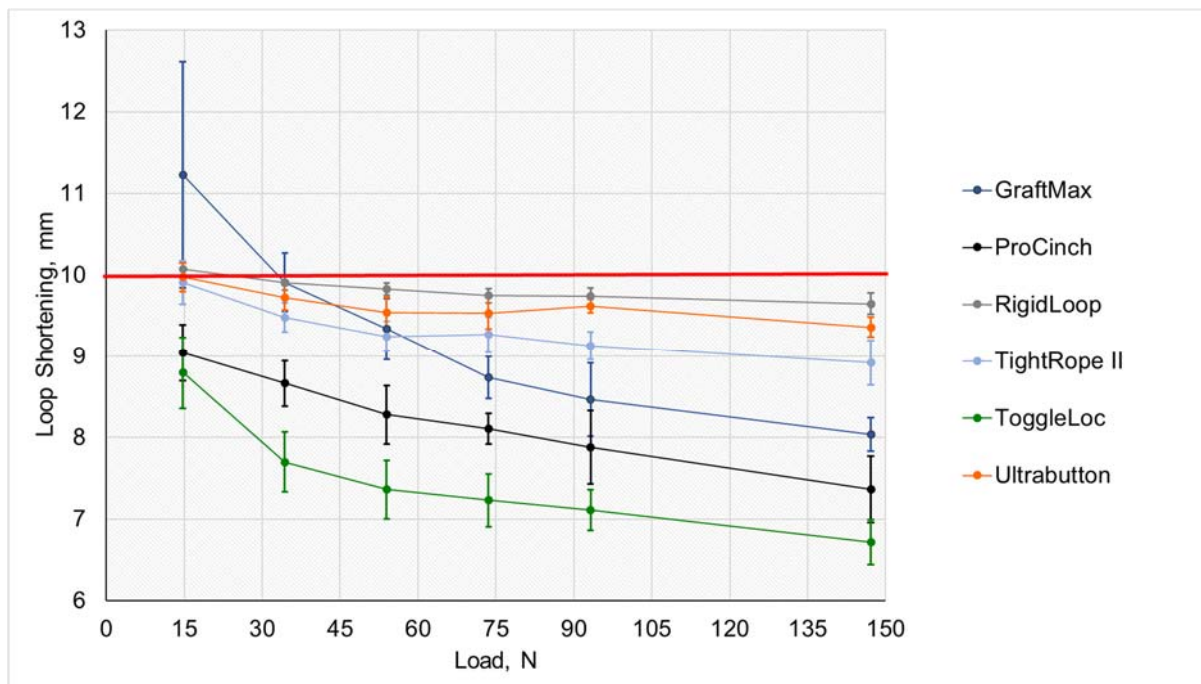


Figure 38: Loop shortening in mm as a function of the load levels for the different testes ALD groups. The shown values are the average of eight measurements and the error bars represent the standard deviation between those measurements. The red line indicates the expected position after the shortening.

In Figure 39 A the position of the button during loop shortening is shown for the *RigidLoop* device. This is representative for all tested groups except the groups of *GraftMax* and *ProCinch*. During loop shortening of *GraftMax* the button is lifted from the disc at the beginning of the shortening process, which leads to a tilted position during actual shortening (see Figure 39 B). At the beginning of the shortening process of the *ProCinch* device, there is a rotational effect of the shortening strands towards the center of the button (see Figure 39 C & D). Panel C shows the initial position before the start of the test is shown, while panel D shows the position of the strands during

the loop shortening. The blue arrow indicates the movement of the suture. For ALDs with a button lock it is observed that, while pulling the shortening strands, the loop running over those strands is lifted from the button. When the shortening strand is unloaded, the loop moves back down until it locks the shortening strands between itself and the button.

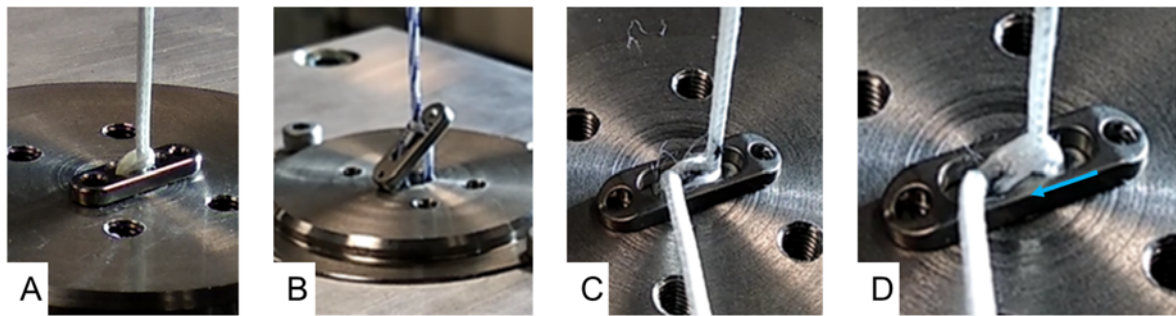


Figure 39: Pictures of the position of the button during the loop shortening, (A) *RigidLoop*, (B) *GraftMax*, (C & D) *ProCinch*. The blue arrow in panel D indicates the movement of the shortening suture toward the center.

The calculated tbb values at the six tested load levels are shown in Figure 40. The ALD *GraftMax* shows an enormous bounce back, compared to the other devices, this is also revealed by the *post hoc Tukey* test, since there is a significant difference in the tbb values between *GraftMax* and all other tested devices at all load levels. *RigidLoop*, *TightRope II*, *ProCinch*, and *UltraButton* show similar values, while *ToggleLoc* has a very small tbb. Furthermore, the fixed loop devices show a tbb close to zero. The calculated mean values with the according standard deviation are shown numerically in appendix II together with the results of the *post hoc Tukey* test.

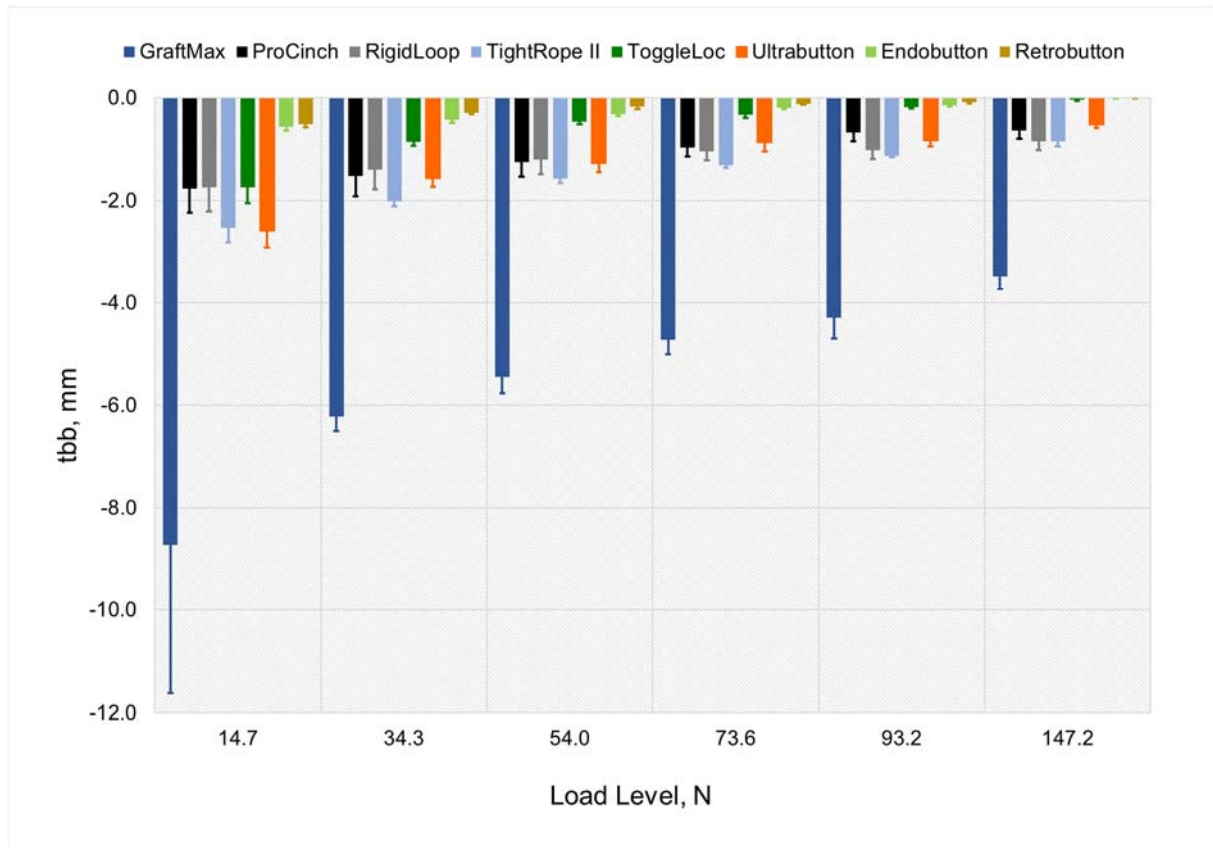


Figure 40: Calculated total bounce back values as a function of the six load levels for the different devices. The shown values are the average of eight measurements and the error bars represent the standard deviation between those measurements.

Finally, the tensioning required to shorten the loops with the testing machine actuator is shown as a function of the weight applied via the hook (see Figure 41). The tensioning values for the ALD *ToggleLoc* are very large compared to those of the other ALDs. The dotted red line indicates a 1:1 transmission ratio and is added to achieve a better comparability. The ALD *Rigidloop* requires significantly less force to be shortened at the last four load levels compared to the other ALDs. The *ProCinch*, *UltraButton* and *TightRope II* groups show similar behavior at all load levels, while *GraftMax* requires slightly more force to be shortened. The average values, including the according standard deviation and the results of the *post hoc Tukey* test are shown numerically in appendix III.

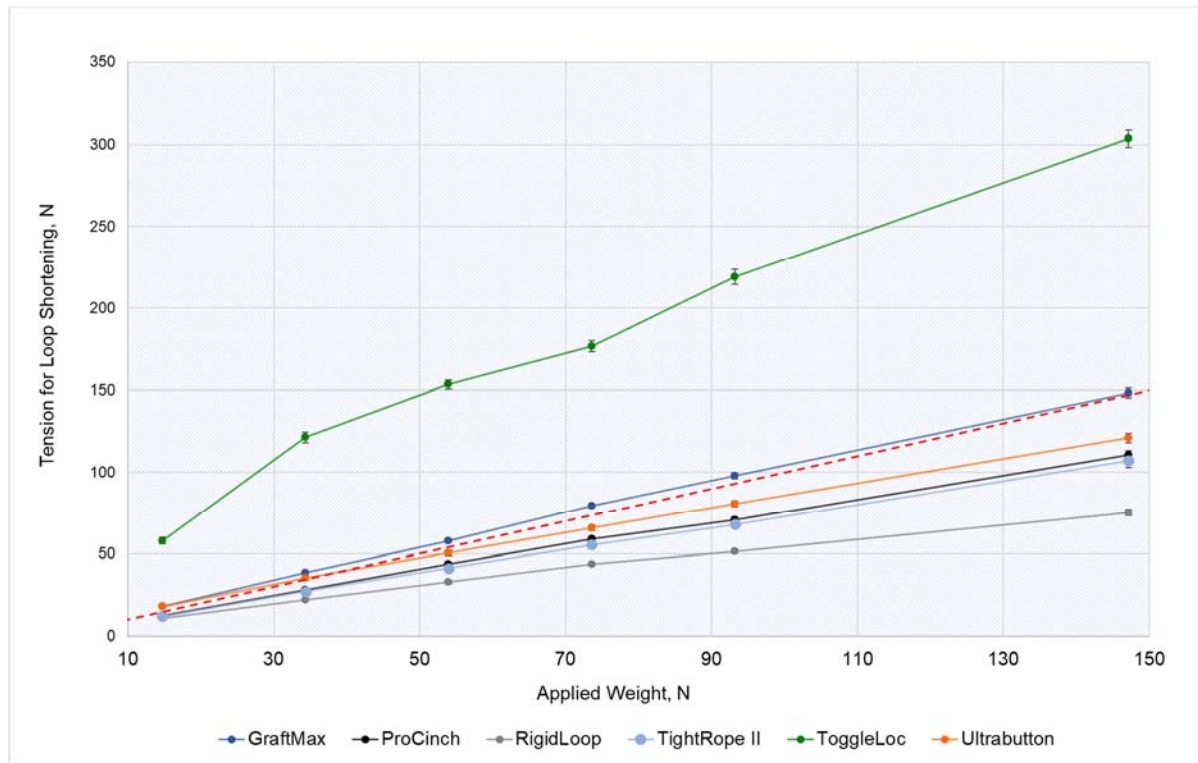


Figure 41: Tensioning force as a function of the applied weight. The red line indicates a 1:1 transmission ratio. The shown values are the average of eight measurements and the error bars represent the standard deviation between those measurements.

4.4. ALD Stability Test

The results of the stability tests are shown in this chapter. First, the displacement of the loop is presented as a function of the number of tested cycles. Thereafter, the cycle numbers at which clinical failure occurs are shown for those devices that reach clinical failure. The last analysis presents the mean elongation after 3000 cycles for the devices that do not reach clinical failure.

The absolute displacement as a function of the number of tested cycles for each of the eight tested groups is presented in Figure 42. The grey lines display the results of the single device test, while the black lines show the results of the device-tendon test series. For a better comparability the clinical failure of 3 mm is marked with a red line. The *ProCinch* group reaches clinical failure within the first 1000 cycles while the *ToggleLoc* devices reach the limit within the first 1500 cycles. *UltraButton* and *GraftMax* also reach clinical failure before the ending of the tests. *Rigidloop* and *TightRope II* show a similar behavior to the two groups of FLDs, *EndoButton* and *RetroButton*, and do not reach clinical failure before the defined test end. Furthermore,

TightRope II, *UltraButton* and *ProCinch* show improved results in the device-tendon test series compared to the single device tests, while *RigidLoop* shows impaired results in this series. The FLDs also show worse results in the device-tendon test series than in the single device tests. The results for *GraftMax* are slightly better in the device-tendon series, while those of *ToggleLoc* show nearly no difference between the two series.

For the single device test the statistical analysis reveals a significant difference ($P \leq 0.05$) between the four device where clinical failure occurs (*GraftMax*, *UltraButton*, *ToggleLoc* and *ProCinch*) and those four devices that reach the defined test end without failing (*EndoButto*, *RetroButton*, *TightRope II* and *RigidLoop*). In contrast to that the *GraftMax* device does not show a significant difference ($P = 0.475$) to *EndoButton*, *RetoButton*, *TightRope II*, and *RigidLoop* in the device-tendon test.

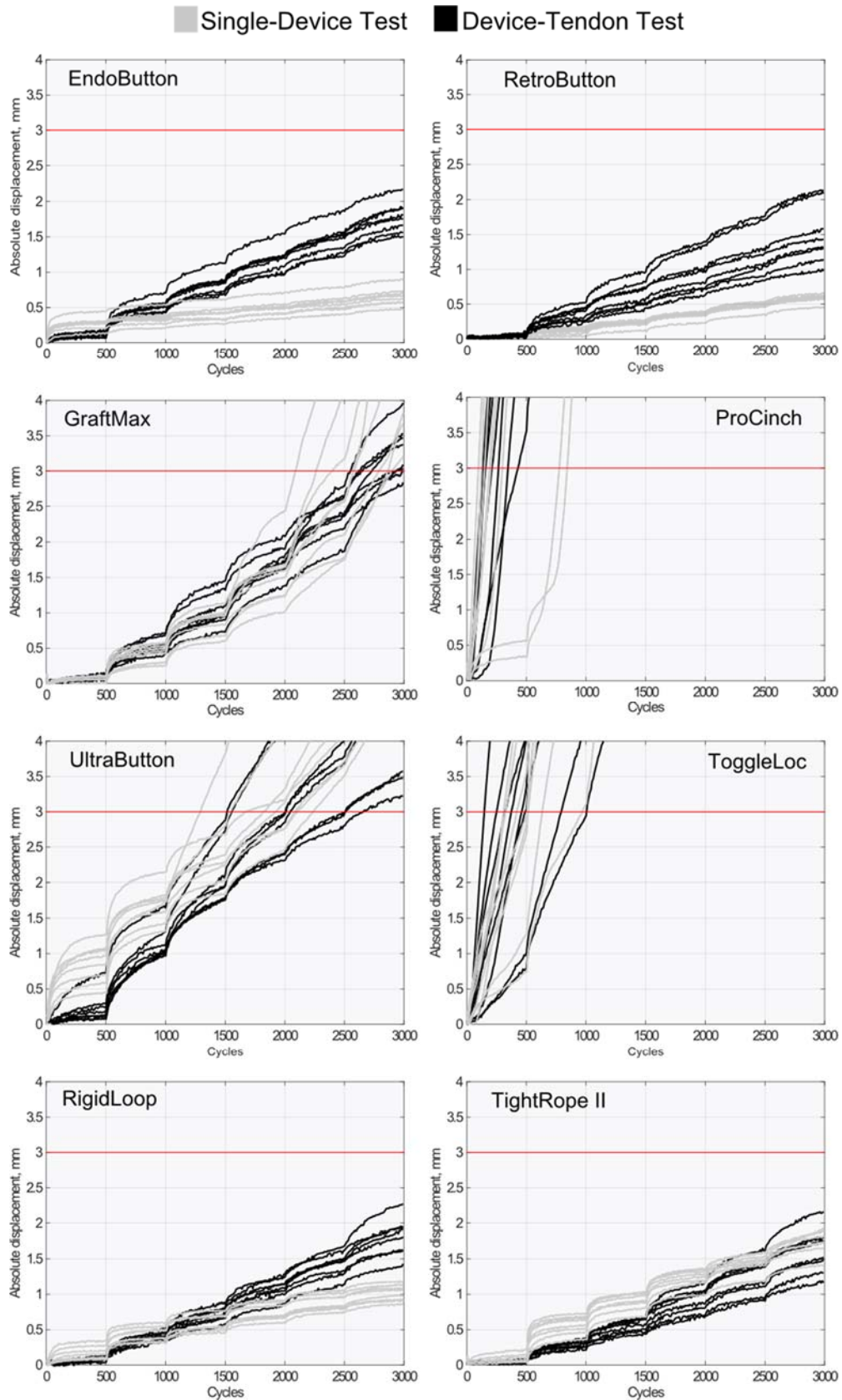


Figure 42: Absolute displacement as a function of the cycles of loading and unloading for each tested group. The results of the single device test series are shown in grey and results of the device-tendon series in black. The red line indicates the clinical failure criteria of 3 mm.

The peak loads at clinical failure as a function of the tested cycles from the single device tests are shown in Figure 43, for those devices that reach clinical failure. 75 % of the *ProCinch* samples reach the limit of 3 mm within the first 500 cycles at a peak load of 50 N. All *ToggleLoc* and *ProCinch* samples fail within the first two load blocks. Clinical failure of the *UltraButton* samples occurs in the peak load range between 150 N and 250 N. Furthermore, 75 % of the *GraftMax* devices reach clinical failure during the last testing block without reaching defined test end.



Figure 43: Peak load at clinical failure as a function of the tested cycles. The results of *GraftMax*, *ProCinch*, *ToggleLoc* and *UltraButton* of the single device test are shown.

Almost all ALDs that reach clinical failure during the single device test, also show early failure in the device-tendon tests (Figure 44). The peak loads at clinical failure of *ProCinch* and *ToggleLoc* are smaller than in the single device test, with a 100 % and 75 % failure rate within the first 500 cycles, respectively. The ALD *UltraButton* shows improved results; 75 % do not fail before the last two load blocks. Furthermore, only six of the eight tested *GraftMax* samples reach clinical failure.

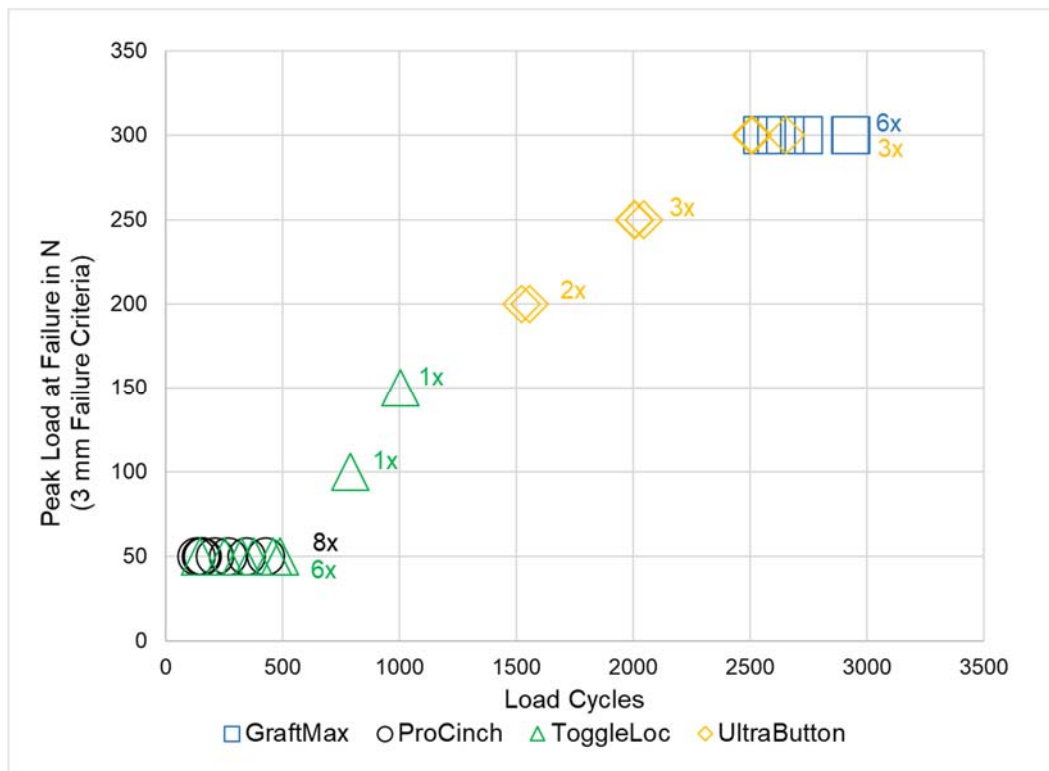


Figure 44: Peak load at clinical failure as a function of the tested cycles. The results of the ALDs *GraftMax*, *ProCinch*, *ToggleLoc* and *UltraButton* of the device-tendon tests are shown.

In Table 6 the mean values and the according standard deviation of the clinical failure cycles are presented for the single device as well as the device-tendon test. *GraftMax* devices pass roughly 200 more cycles in the device-tendon test, than in the single device test. *ProCinch* fails roughly 100 cycles earlier in the device-tendon test than in the single device test. Furthermore, the *GraftMax* and *UltraButton* groups have a broad variation of clinical failure in the single device test, this is shown by the high standard deviation. On the other hand, the groups of *UltraButton* and *ToggleLoc* show a wide intragroup variation in the device-tendon test.

Table 6: Overview of the mean values of the cycles of clinical failure and the according standard deviation cycles. Including the results of the single device test and of the Device-Tendon test.

device	cycle of clinical failure, mean \pm SD	
	single device	device-tendon
<i>GraftMax</i>	2607 \pm 269	2801 \pm 184
<i>UltraButton</i>	1832 \pm 318	2100 \pm 429
<i>ToggleLoc</i>	520 \pm 210	480 \pm 285
<i>ProCinch</i>	329 \pm 230	230 \pm 107

The p-values of the *post hoc Tukey* test of the cycles of clinical failure reveal a significant difference between all tested groups with exception of *ProCinch* and *ToggleLoc* for both test series (see Table 7).

Table 7: Results of the *post hoc Tukey* test of the cycles of clinical failure. The results for the single device test and for the device-tendon test are shown.

single device test	GraftMax	UltraButton	ToggleLoc	ProCinch
<i>GraftMax</i>	-	<0.001	<0.001	<0.001
<i>UltraButton</i>	<0.001	-	<0.001	<0.001
<i>ToggleLoc</i>	<0.001	<0.001	-	0.526
<i>ProCinch</i>	<0.001	<0.001	0.526	-
device tendon test	GraftMax	UltraButton	ToggleLoc	ProCinch
<i>GraftMax</i>	-	<0.001	<0.001	<0.001
<i>UltraButton</i>	<0.001	-	<0.001	<0.001
<i>ToggleLoc</i>	<0.001	<0.001	-	0.204
<i>ProCinch</i>	<0.001	<0.001	0.204	-

The elongation after 3000 cycles for *EndoButton*, *RetroButton*, *TightRope II* and *Rigidloop* is presented in Table 8. The fixed loop devices *EndoButton* and *RetroButton* present a similar elongation, which is less than the elongation of the two ALDs in the single device test series. *Rigidloop* shows a smaller average elongation than *TightRope II* in the single device test, while the results in the device-tendon test are inverted.

Table 8: Mean elongation and standard deviation of eight measurements. The results of the ALDs, that do not reach clinical failure and the FLDs after 3000 cycles of loading and complete unloading are shown.

	mean elongation after 3000 cycles	
device	single device in mm	device - tendon in mm
<i>EndoButton</i>	0.655 ± 0.129	1.799 ± 0.208
<i>RetroButton</i>	0.549 ± 0.060	1.436 ± 0.352
<i>RigidLoop</i>	1.021 ± 0.114	1.827 ± 0.257
<i>TightRope II</i>	1.754 ± 0.168	1.554 ± 0.234

The results of the *post hoc Tukey* test for the mean elongation after 3000 cycles are shown in Table 9. For the single device test the results are significantly different with exception of the two fixed loop devices. The values of the device-tendon test only show a significant difference between *RigidLoop* and *RetroButton*.

Table 9: Results of the *post hoc Tukey* test for comparison of the elongation after 3000 cycles. The results for the single device tests and the device-tendon tests are shown.

single device test	EndoButton	RetroButton	Rigidloop	TightRope II
<i>EndoButton</i>	-	0.334	<0.001	<0.001
<i>RetroButton</i>	0.334	-	<0.001	<0.001
<i>Rigidloop</i>	<0.001	<0.001	-	<0.001
<i>TightRope II</i>	<0.001	<0.001	<0.001	-
device-tendon test	EndoButton	RetroButton	Rigidloop	TightRope II
<i>EndoButton</i>	-	0.053	0.997	0.282
<i>RetroButton</i>	0.053	-	0.033	0.816
<i>Rigidloop</i>	0.997	0.033	-	0.199
<i>TightRope II</i>	0.282	0.816	0.199	-

5. Discussion

In this chapter all the results presented in chapter four are discussed. Firstly, the results of the investigated development process and the possibilities of the conformity assessment procedures according to the MDR are discussed. In continuation, the results of the three biomechanical test series are discussed. As this testing method is supposed to become a basis for a standardized method, all critical performance aspects of the ALDs have to be considered thoroughly.

Development Process

The analysis of the development process of *TightRope II* (Arthrex, USA), provides an overview over the most important development steps. Several steps, which have been performed in the development of the already existing *TightRope*, can be adapted and used for the new product. Therefore, the workload is reduced considerably. During this process, the design traceability matrix is a helpful tool, where all the information of the different steps are documented and can be viewed by everyone associated with the project. *TightRope II* is classified as class IIb product as presented in chapter four. The classification is essential for the analysis of the possible conformity assessment procedures, since the possibilities depend on the class of the device. The challenges, which are observed during the analysis of the possibilities, are described in the following paragraph.

One of the biggest issues is that, within the product verification according to annex XI part B of the MDR, batch test are not allowed. This is especially challenging for smaller companies without a complete quality management system, since each produced device has to be tested separately, which leads to much higher costs. Overall, this means that with the new medical device regulation, the manufacturer is forced more and more to implement a complete QMS system, which involves a lot of effort and high fixed costs. Another striking aspect is that so far there is hardly any notified body which could perform the conformity assessment according to the MDR, although the new medical device regulation has already been implemented in May 2017. Therefore, it can be expected that as soon as the medical devices have to be certified according to the MDR there will be very long waiting times.

Pre-Testing of *Polished* and *Non-Polished TightRope II* Buttons

A major aspect within the development process is the decision whether to use the *polished* or *non-polished* version of the button. Therefore, the biomechanical test results of those two groups are analyzed separately. Since, for the *polished* button, an additional post-processing step is necessary, the production of the *non-polished* button is cheaper, which would be in favor of the *non-polished* version. The results of the loop shortening tests do not show a significant difference between the two groups. In contrast to that, the stability single device test shows a difference of the absolute displacement after 3000 loading and unloading cycles. Therefore, the engineering team prefers the *polished* over the *non-polished* version and thus accepts the higher production costs. For that reason, the *non-polished* group is excluded from the following overall comparison to the competitor devices.

ALD Loop Shortening

The analysis of the shortening accuracy reveals a similar, satisfying shortening behavior for the *RigidLoop*, *TightRope II*, and *UltraButton* devices, since a shortening close to 10 mm is reached. In contrast, the groups of *ProCinch*, *ToggleLoc* and *GraftMax* show a significantly worse behavior (Figure 38). *ToggleLoc* and *ProCinch* have an insufficient shortening behavior since the shortening length is far below the expected 10 mm. *ToggleLoc* is the only device that uses an antegrade shortening mechanism and where all sutures run through the same hole in the button (see Figure 20). Therefore, the force required for the shortening is higher due to more friction, which may be the reason for the worse shortening behavior. The poor shortening behavior of *ProCinch* is induced by the rotation movement of the suture, which occurs at the beginning of the shortening process (see Figure 39 C & D). The actual shortening of the loop starts after the rotation of the shortening strand, therefore the expected 10 mm cannot be reached. The *GraftMax* group is shortened by more than the expected 10 mm at the first load level. When the shortening strand is pulled, an initial lift of the button occurs (see Figure 39 B). Therefore, the actual loop shortening starts delayed and the specified transmission ration is not correct anymore. With increasing load levels, the tilting of the button decreases and therefore the shortening length is reduced. All devices show that, the achieved shortening length decreases with

increasing load levels, this is caused by a greater stretching of the shortening sutures when higher loads are applied (see Figure 38).

The total bounce back of the *GraftMax* group is significantly higher than for the other tested groups. Those high tbb values also result from the above described initial tilting of the button, since the tilting of the button is reversed when the shortening strand is unloaded. For the devices using a button lock (*GraftMax*, *RigidLoop*, and *TightRope II*), the lifting of the loop during the shortening process has an influence on the tbb. When unloading the shortening strands the loop moves back onto the button. This leads to an initial elongation of the loop until the locking mechanism holds. With an increasing load level the total bounce back decreases. This behavior can be identified for all devices and results from the decreasing weight difference to the maximum load that is applied at the end of the test. The *ToggleLoc* group shows a comparably low tbb that also results from the design of the button and the associated higher friction. Since the FLDs *EndoButton* and *RetroButton* do not include a locking mechanism, the tbb is only induced by stretching of the sutures. Therefore, the recorded tbb is small at lower load levels and close to zero at the last load level.

The analysis of the forces required to shorten the loops reveals a significant difference between the *ToggleLoc* group and all other tested groups at all load levels (see Figure 41). The high force values for the tensioning of *ToggleLoc* occur because of the above-mentioned design of the button and the antegrade shortening (see Figure 20 C) mechanism. The groups of *GraftMax*, *ProCinch*, *RigidLoop*, *TightRope II*, and *UltraButton* show a better behavior, since they show a better ratio between tensioning force and applied weight. However, *RigidLoop* requires less tensioning force than the other tested ALDs at higher load levels, while *GraftMax* requires more tensioning force at higher load levels.

As of now, there is no previous study that focuses on the analysis of the shortening behavior of ALDs. Therefore, the obtained test results and used methods of this study are pertinent to the continuous improvement of current ACL reconstruction fixing devices and techniques that aim to restore normal function of the knee joint.

ALD Stability Test

The single device test series represents a worst-case scenario since the metallic components used in the test setup lead to a direct transmission of the forces into the loop. In contrast, the device-tendon test series is intended to represent the behavior of the ALDs in an environment that resembles that of the clinical application more closely. A difference in the results is expected since the tendon has a more elastic behavior, which dampens the forces applied to the loop.

The devices are tested under cyclic loading and complete unloading situations. Due to the complete unloading a different outcome depending on the locking mechanism of the ALDs is expected. The results presented in Figure 42 show that the groups of *GraftMax*, *ProCinch*, *UltraButton*, and *ToggleLoc* reach an elongation of 3 mm, which is defined as clinical failure, before the end of the test. The groups of *EndoButton*, *RetroButton*, *RigidLoop*, and *TightRope II*, on the other hand, do not reach this elongation value. The *ProCinch* group shows the worst results since all samples fail within the first 500 cycles. The *ToggleLoc* group shows similar poor results. Glasbrenner et al. [74] evaluated whether ALDs with a locking mechanism based on a chinese finger trap resist cyclic loading and complete unloading. They determined significantly worse results for ALDs with a locking mechanism based on a CFT than for ALDs with a button lock. Since *ProCinch*, *UltraButton* and *ToggleLoc* are the only tested devices, with a locking mechanism based only on a CFT, the same observation can be made here. Even though the *UltraButton* device has the same locking mechanism as *ProCinch* and *ToggleLoc* it reaches clinical failure later, which is caused by the higher transmission ratio. For the *ProCinch* and *ToggleLoc* devices, there is no significant difference between the single device results and the device tendon results. The *UltraButton* and *GraftMax* groups show a better behavior in the device tendon test than in the single device test, however the devices still fail before completing 3000 cycles. The fact that the ALD *GraftMax* is the only device using just the button lock with a transmission ratio of 2:1, is presumed to cause the high elongation. Furthermore, it can be stated that the complete unloading during the cyclic testing has a major influence on the test results. Ahmad et al. [10] reported that the devices *ProCinch* and *Ultrabutton* do not reach clinical failure within their 2000 cycle protocol. However, their protocol does not include complete unloading, which could be the reason for the different results as a remaining minimum of load may improve the stability of an ALD.

From the six tested ALD groups, only *TightRope II* and *RigidLoop* do not reach clinical failure. In the single device test *RigidLoop* shows less absolute displacement than *TightRope II* (see Table 8). However, in the device tendon test the *Rigidloop* group shows a greater mean value of the absolute displacement. The results of the device-tendon test show that implementing the tendon into the test has a positive effect on the stability of the ALD *TightRope II*. However, this effect is reversed for the ALD *RigidLoop*. It can be assumed that this difference occurs due to the different locking mechanisms of the two devices. The locking mechanism of *TightRope II* is based on a combination of CFT and button lock, while *RigidLoop* is only based on a button lock and two loops running over the button. Therefore, it can be stated that the flexible behavior of the tendon, which is given in the clinical application, affects the biomechanical stability of the devices. Furthermore, the different number of strands may be an influencing factor, since *TightRope II* has only four strands while *RigidLoop* has eight strands. It is assumed that a smaller number of strands reduces the risk of slack in some of the strands, which could lead to a higher displacement. Despite the different number of strands, the transmission ratio for the shortening is the same for both devices.

The elongation of the fixed loop devices in the single device test is significantly smaller than that of the tested ALDs. Barrow et al. [9] reported the same result comparing the FLD *EndoButton* to the ALDs *ToggleLoc* and *TightRope* in their studies. However, the device-tendon test does not show a significant difference between *TightRope II* and the FLDs. In contrast, *RigidLoop* does show significantly more elongation compared to the fixed loop device *RetroButton* in the device-tendon test. These results indicate a major advantage of the new device *TightRope II* compared to the other tested ALDs. In conclusion, it can be stated that *TightRope II* is an improved version of *TightRope*, since the disadvantage in the stability test of *TightRope*, described by Ahmad et al. [10] and Barrow et al. [9] is corrected in the new product.

6. Conclusion

The aim of this thesis is to analyze the development process, the possible conformity assessment procedures for the new medical device *TightRope II* (Arthrex, USA) according to the MDR and to perform a biomechanical comparison between the new device and the most important competitor devices.

The ALD *TightRope II* is classified as class IIb product according to the MDR. Thereafter, the possible ways to perform the conformity assessment, which is mandatory for the CE certification for a class IIb product, are identified.

The pre-tests performed within the development process show a superior biomechanical behavior for the *polished* version of the *TightRope II* button as compared to the *non-polished* version. Therefore, the *polished* version is preferred.

The biomechanical comparison of the adjustable loop devices reveals that *RigidLoop* and *TightRope II* are the only devices that do not reach clinical failure. These devices even show a behavior similar to the fixed loop devices *EndoButton* and *RetroButton*, which are tested as reference groups. In conclusion, the test results show that a combination of two locking mechanisms leads to an improved stability of the loop.

The implemented testing protocols for all test series allow for a critical evaluation of different available ALDs on the market, with a good comparability between the tested groups. In comparison to the previously performed studies, a complete unloading is applied in the stability tests, which allows for a detailed examination of the ALDs locking mechanisms in dynamically loaded test situations. Furthermore, the shortening behavior of the ALDs is analyzed in this study. This reveals important aspects, such as the shortening accuracy and settling effects of the loops, that are not found in previous studies. Therefore, the used test protocol can be recommended for further testing. As the implementation of the tendon reveals a significantly different outcome of the results in the stability tests, it should be considered to add a tendon to the tensioning test series, in order to perform this series in an environment closer to the clinical application.

Literature

- [1] M. M. M. Kiapour A.M., "Basic science of anterior cruciate ligament injury and repair," *Bone & Joint Research*, vol. 3, 2014.
- [2] T. E. Hewett, S. L. Di Stasi, and G. D. Myer, "Current concepts for injury prevention in athletes after anterior cruciate ligament reconstruction," (in eng), *The American journal of sports medicine*, vol. 41, no. 1, pp. 216-24, Jan 2013.
- [3] H. Wildhalm, "Kreuzbandriss," *ÖÄZ*, 2017.
- [4] H. S. Kim, J. K. Seon, and A. R. Jo, "Current trends in anterior cruciate ligament reconstruction," *Knee Surg Relat Res*, vol. 25, no. 4, pp. 165-73, Dec 2013.
- [5] N. A. Mall *et al.*, "Incidence and trends of anterior cruciate ligament reconstruction in the United States," *The American journal of sports medicine*, vol. 42, no. 10, pp. 2363-70, Oct 2014.
- [6] S. E. S. U. Schünke M., Voll M. Wesker K., *Prometheus*. Stuttgart: Georg Thieme Verlag, 2014.
- [7] Z. T. Petersen W., *Das vordere Kreuzband Grundlagen und aktuele Praxis der operativen therapie*. Köln: Deutscher Ärzte-Verlag, 2009.
- [8] P. Mahapatra, S. Horriat, and B. S. Anand, "Anterior cruciate ligament repair - past, present and future," *J Exp Orthop*, vol. 5, no. 1, p. 20, Jun 15 2018.
- [9] A. E. Barrow, M. Pilia, T. Guda, W. R. Kadrmas, and T. C. Burns, "Femoral suspension devices for anterior cruciate ligament reconstruction: do adjustable loops lengthen?," *The American journal of sports medicine*, vol. 42, no. 2, pp. 343-9, Feb 2014.
- [10] S. S. Ahmad *et al.*, "Adjustable loop ACL suspension devices demonstrate less reliability in terms of reproducibility and irreversible displacement," (in eng), *Knee surgery, sports traumatology, arthroscopy : official journal of the ESSKA*, vol. 26, no. 5, pp. 1392-1398, May 2018.
- [11] W. Platzer, *Taschenatlas Anatomie Band 1 Bewegungsapparat*. Thieme, 2009.
- [12] A. Faller and M. Schünke, *Der Körper des Menschen: Einführung in Bau und Funktion*, 15th ed. Stuttgart: Georg Thieme Verlag, 2008.
- [13] M. Wagner, *Funktionelle Anatomie des Kniegelenks*. Springer Verlag, 1987.
- [14] A. Prescher, "Anatomie des Kniegelenks (Articulatio genus)," in *AE-Manual der Endoprothetik*: Springer, 2011, pp. 1-18.
- [15] B. S. R. Gaillard, R. Ballis, P. Neyret and S. Lustig, "Anatomy, Physiology, and Biomechanics of the Native Knee In: Total Knee Arthroplasty- A Comprehensive Guide," Springer, 2015, pp. 1-25.
- [16] V. B. Duthon, C. Barea, S. Abrassart, J. H. Fasel, D. Fritschy, and J. Menetrey, "Anatomy of the anterior cruciate ligament," (in eng), *Knee surgery, sports traumatology, arthroscopy : official journal of the ESSKA*, vol. 14, no. 3, pp. 204-13, Mar 2006.
- [17] G. Li, L. E. DeFrate, H. E. Rubash, and T. J. Gill, "In vivo kinematics of the ACL during weight-bearing knee flexion," (in eng), *Journal of orthopaedic research : official publication of the Orthopaedic Research Society*, vol. 23, no. 2, pp. 340-4, Mar 2005.
- [18] N. Relph, L. Herrington, and S. Tyson, "The effects of ACL injury on knee proprioception: a meta-analysis," (in eng), *Physiotherapy*, vol. 100, no. 3, pp. 187-95, Sep 2014.
- [19] H. A. Richard and G. Kullmer, *Biomechanik: Grundlagen und Anwendungen auf den menschlichen Bewegungsapparat*. Springer-Verlag, 2014.
- [20] M. Jagodzinski, N. Friederich, and W. Müller, *Das Knie: Form, Funktion und ligamentäre Wiederherstellungschirurgie*. Springer-Verlag, 2016.
- [21] V. Pinskerova *et al.*, "Does the femur roll-back with flexion?," *The Journal of bone and joint surgery. British volume*, vol. 86, no. 6, pp. 925-931, 2004.
- [22] S. L. Woo, R. E. Debski, J. D. Withrow, and M. A. Jansushek, "Biomechanics of knee ligaments," (in eng), *The American journal of sports medicine*, vol. 27, no. 4, pp. 533-43, Jul-Aug 1999.

- [23] C. Domnick, M. J. Raschke, and M. Herbolt, "Biomechanics of the anterior cruciate ligament: Physiology, rupture and reconstruction techniques," *World journal of orthopedics*, vol. 7, no. 2, pp. 82-93, 2016.
- [24] K. A. Taylor *et al.*, "In vivo measurement of ACL length and relative strain during walking," *Journal of biomechanics*, vol. 46, no. 3, pp. 478-483, 2013.
- [25] S. Bachmaier, P. A. Smith, J. Bley, and C. A. Wijdicks, "Independent Suture Tape Reinforcement of Small and Standard Diameter Grafts for Anterior Cruciate Ligament Reconstruction: A Biomechanical Full Construct Model," (in eng), *Arthroscopy*, vol. 34, no. 2, pp. 490-499, Feb 2018.
- [26] R. G. Marx, *Revision ACL reconstruction: indications and technique*. Springer, 2013.
- [27] R. Schabus and E. Bosina, *Das Knie: Diagnostik–Therapie–Rehabilitation*. Springer-Verlag, 2007.
- [28] D. E. Meuffels *et al.*, "Guideline on anterior cruciate ligament injury," *Acta orthopaedica*, vol. 83, no. 4, pp. 379-386, 2012.
- [29] H. Louboutin *et al.*, "Osteoarthritis in patients with anterior cruciate ligament rupture: a review of risk factors," *Knee*, vol. 16, no. 4, pp. 239-44, Aug 2009.
- [30] M. F. Sherman, L. Lieber, J. R. Bonamo, L. Podesta, and I. Reiter, "The long-term followup of primary anterior cruciate ligament repair. Defining a rationale for augmentation," (in eng), *The American journal of sports medicine*, vol. 19, no. 3, pp. 243-55, May-Jun 1991.
- [31] K. M. Sutton and J. M. Bullock, "Anterior cruciate ligament rupture: differences between males and females," *J Am Acad Orthop Surg*, vol. 21, no. 1, pp. 41-50, Jan 2013.
- [32] G. S. DiFelice, C. Villegas, and S. Taylor, "Anterior Cruciate Ligament Preservation: Early Results of a Novel Arthroscopic Technique for Suture Anchor Primary Anterior Cruciate Ligament Repair," *Arthroscopy*, vol. 31, no. 11, pp. 2162-71, Nov 2015.
- [33] R. Crawford, G. Walley, S. Bridgman, and N. Maffulli, "Magnetic resonance imaging versus arthroscopy in the diagnosis of knee pathology, concentrating on meniscal lesions and ACL tears: a systematic review," (in eng), *British medical bulletin*, vol. 84, pp. 5-23, 2007.
- [34] J. W. Katz and R. J. Fingerhuth, "The diagnostic accuracy of ruptures of the anterior cruciate ligament comparing the Lachman test, the anterior drawer sign, and the pivot shift test in acute and chronic knee injuries," (in eng), *The American journal of sports medicine*, vol. 14, no. 1, pp. 88-91, Jan-Feb 1986.
- [35] A. Benjaminse, A. Gokeler, and C. P. van der Schans, "Clinical diagnosis of an anterior cruciate ligament rupture: a meta-analysis," *J Orthop Sports Phys Ther*, vol. 36, no. 5, pp. 267-88, May 2006.
- [36] M. Prins, "The Lachman test is the most sensitive and the pivot shift the most specific test for the diagnosis of ACL rupture," (in eng), *The Australian journal of physiotherapy*, vol. 52, no. 1, p. 66, 2006.
- [37] A. Leumann *et al.*, "Behandlung der vorderen Kreuzbandruptur im Sport: State of the Art in der Indikationsstellung," *Schweizerische Zeitschrift für Sportmedizin und Sporttraumatologie*, vol. 61, no. 2, pp. 7-10, 2013.
- [38] C. Voigt, M. Schönaich, and H. Lill, "Anterior Cruciate Ligament Reconstruction: State of the Art," *European Journal of Trauma*, journal article vol. 32, no. 4, pp. 332-339, August 01 2006.
- [39] P. Delincé and D. Ghafil, "Anterior cruciate ligament tears: conservative or surgical treatment? A critical review of the literature," *Knee Surgery, Sports Traumatology, Arthroscopy*, journal article vol. 20, no. 1, pp. 48-61, January 01 2012.
- [40] M. M. Murray, "History of ACL treatment and current gold standard of care," in *The ACL Handbook*: Springer, 2013, pp. 19-28.
- [41] C. s. H. Colorado. (05.02.2019). *Children's Hospital Colorado - ACL Graft Options* [Online]. Available: <https://www.childrenscolorado.org/conditions-and-advice/sports-articles/sports-injuries/acl-graft-options/>.
- [42] M. Xu *et al.*, "Outcomes of anterior cruciate ligament reconstruction using single-bundle versus double-bundle technique: meta-analysis of 19 randomized controlled trials," (in eng), *Arthroscopy*, vol. 29, no. 2, pp. 357-65, Feb 2013.

- [43] C. Aga, K. J. Wilson, S. Johansen, G. Dornan, R. F. La Prade, and L. Engebretsen, "Tunnel widening in single- versus double-bundle anterior cruciate ligament reconstructed knees," *Knee Surgery, Sports Traumatology, Arthroscopy*, journal article vol. 25, no. 4, pp. 1316-1327, April 01 2017.
- [44] O. Chechik, E. Amar, M. Khashan, R. Lador, G. Eyal, and A. Gold, "An international survey on anterior cruciate ligament reconstruction practices," *International Orthopaedics*, journal article vol. 37, no. 2, pp. 201-206, February 01 2013.
- [45] B. C. Noonan, J. S. Dines, A. A. Allen, D. W. Altchek, and A. Bedi, "Biomechanical Evaluation of an Adjustable Loop Suspensory Anterior Cruciate Ligament Reconstruction Fixation Device: The Value of Retensioning and Knot Tying," (in eng), *Arthroscopy*, vol. 32, no. 10, pp. 2050-2059, Oct 2016.
- [46] D. D. Nye, W. R. Mitchell, W. Liu, and R. V. Ostrander, "Biomechanical Comparison of Fixed-Loop and Adjustable-Loop Cortical Suspensory Devices for Metaphyseal Femoral-Sided Soft Tissue Graft Fixation in Anatomic Anterior Cruciate Ligament Reconstruction Using a Porcine Model," *Arthroscopy*, vol. 33, no. 6, pp. 1225-1232 e1, Jun 2017.
- [47] B. D. Beynon, R. J. Johnson, J. A. Abate, B. C. Fleming, and C. E. Nichols, "Treatment of anterior cruciate ligament injuries, part I," (in eng), *The American journal of sports medicine*, vol. 33, no. 10, pp. 1579-602, Oct 2005.
- [48] F. S. Kamelger, U. Onder, W. Schmoelz, K. Tecklenburg, R. Arora, and C. Fink, "Suspensory fixation of grafts in anterior cruciate ligament reconstruction: a biomechanical comparison of 3 implants," (in eng), *Arthroscopy*, vol. 25, no. 7, pp. 767-76, Jul 2009.
- [49] P. Kousa, T. L. Jarvinen, M. Vihavainen, P. Kannus, and M. Jarvinen, "The fixation strength of six hamstring tendon graft fixation devices in anterior cruciate ligament reconstruction. Part I: femoral site," (in eng), *The American journal of sports medicine*, vol. 31, no. 2, pp. 174-81, Mar-Apr 2003.
- [50] M. Kokkinakis, A. Ashmore, and M. El-Guindi, "Intraoperative complications using the Bio-Transfix femoral fixation implant in anterior cruciate ligament reconstruction," (in eng), *Archives of orthopaedic and trauma surgery*, vol. 130, no. 3, pp. 375-9, Mar 2010.
- [51] H. Ozer and A. Oznur, "Complications following hamstring anterior cruciate ligament reconstruction with femoral cross-pin fixation," (in eng), *Arthroscopy*, vol. 21, no. 11, pp. 1407-8; author reply 1408, Nov 2005.
- [52] S. U. Scheffler, N. P. Sudkamp, A. Gockenjan, R. F. Hoffmann, and A. Weiler, "Biomechanical comparison of hamstring and patellar tendon graft anterior cruciate ligament reconstruction techniques: The impact of fixation level and fixation method under cyclic loading," (in eng), *Arthroscopy*, vol. 18, no. 3, pp. 304-15, Mar 2002.
- [53] D. M. Stadelmaier, W. R. Lowe, O. A. Ilahi, P. C. Noble, and H. W. Kohl, 3rd, "Cyclic pull-out strength of hamstring tendon graft fixation with soft tissue interference screws. Influence of screw length," (in eng), *The American journal of sports medicine*, vol. 27, no. 6, pp. 778-83, Nov-Dec 1999.
- [54] C. S. Ahmad, T. R. Gardner, M. Groh, J. Arnouk, and W. N. Levine, "Mechanical properties of soft tissue femoral fixation devices for anterior cruciate ligament reconstruction," *The American journal of sports medicine*, vol. 32, no. 3, pp. 635-40, Apr-May 2004.
- [55] A. I. N. Florida). *BioComposite Interference Screws*, LA1-0150-EN_E, 2018.
- [56] F. Arthrex Inc.(Naples. *Bio-TransFix ACL Reconstruction Surgical Technique*, LT1-0120-20-EN_K, 2017.
- [57] F. Arthrex Inc.(Naples. *TightRope Attachable Button System (ABS) Implant All-Inside ACL Reconstruction - Surgical Technique*, LT1-0158-EN-C, 2018.
- [58] F. Arthrex Inc.(Naples. *GraftLink ACL Reconstruction With Brace Ligament Augmentation Surgical Technique*, LT1-00120-EN_A, 2019.
- [59] *ACL TightRope RT, Advancing ACL TightRope Fixation in a New Direction*, 2010.
- [60] B. Medizntechnologie. *Der lange Weg eines Medizinprodukts von der Idee bis zur Anwendung am Patienten*, 2016.

- [61] C. Baumgartner, "Medizinprodukterecht: Die wichtigsten gesetzlichen Rahmenbedingungen für Medizinprodukte-Hersteller und Betreiber in Österreich und Europa, Vorlesungsfolien," *TU Graz, HCE*, 2018.
- [62] *REGULATION (EU) 2017/745 OF THE EUROPEAN PARLIAMENT AND OF THE COUNCIL of 5 April 2017 on medical devices, amending Directive 2001/83/EC, Regulation (EC) No 178/2002 and Regulation (EC) No 1223/2009 and repealing Council Directives 90/385/EEC and 93/42/EEC*, T. E. P. A. O. T. COUNCIL, 2017.
- [63] *ÖVE/ÖNORM EN ISO 13485: 2016 07 01 - Medizinprodukte - Qualitätsmanagementsysteme- Anforderungen für regulatorische Zwecke*, 2016.
- [64] *ÖVE/ÖNORM EN ISO 14971:2013 03 01 - Medizinprodukte - Anwendung des Risikomanagements auf Medizinprodukte*, 2013.
- [65] B. S. Medicine. *Biomet Sports Medicine ToggleLoc System*, 01-50-1186 Revision C ed., 2014.
- [66] smith&nephew. *Ultrabutton™ Adjustable Fixation Device*, Rev. A 02/16 ed., 2016.
- [67] Stryker. *ProCinch™ with IntelliBraid Technology Reference Guide 1000901896 Rev. A ed.*, 2015.
- [68] Stryker. *Stryker ProCinch™*, 234-102-090 ed., 2015.
- [69] D. M. S. Medicine. *RIGIDLOOP™ Adjustable Cortical Fixation System 111882 Rev:D ed.*, 2014.
- [70] C. Linvatec. *Instructions for Use for GraftMax™ Button ALB REV AB ed.*, 2015.
- [71] C. Corporation. *GraftMax Button-Adjustable Cortical Fixation Device*.
- [72] ConMed. (07.03.2019). *GraftMaxButton Design and Function - Product Video* [Online]. Available:
<http://www.conmed.com/layouts/MediaFramework/Sublayouts/Player.aspx?itemId=A5268FE3C6223BCAB1AD715B86C5575D&playerId=337236E7E48C4941823CF2D3528A96A3&width=640&height=360>.
- [73] E. Monaco, S. Bachmaier, M. Fabbri, R. M. Lanzetti, C. A. Wijdicks, and A. Ferretti, "Intraoperative Workflow for All-Inside Anterior Cruciate Ligament Reconstruction: An In Vitro Biomechanical Evaluation of Preconditioning and Knot Tying," *Arthroscopy*, vol. 34, no. 2, pp. 538-545, Feb 2018.
- [74] J. Glasbrenner *et al.*, "Adjustable buttons for ACL graft cortical fixation partially fail with cyclic loading and unloading," *Knee surgery, sports traumatology, arthroscopy : official journal of the ESSKA*, Oct 27 2018.
- [75] C. Domnick *et al.*, "Evaluation of biomechanical properties: are porcine flexor tendons and bovine extensor tendons eligible surrogates for human tendons in in vitro studies?," *Archives of orthopaedic and trauma surgery*, journal article vol. 136, no. 10, pp. 1465-1471, October 01 2016.
- [76] N. Arnout, J. Myncke, J. Vanlauwe, L. Labey, D. Lismont, and J. Bellemans, "The influence of freezing on the tensile strength of tendon grafts : a biomechanical study," (in eng), *Acta orthopaedica Belgica*, vol. 79, no. 4, pp. 435-43, Aug 2013.
- [77] *ARAMIS User Manual - Software*, rev-c ed., rev-c.

Figures

Figure 1: Anatomy of the bones of the right knee: Anterior view (A), posterior view (B) and lateral view (C). The figure has been modified from ref. [6].	2
Figure 2: Medial view of the knee joint. The figure has been modified from ref. [6].	3
Figure 3: Tibia-plateau with meniscus medialis and lateralis. The figure has been modified from ref. [6].	4
Figure 4: Schematic of the collateral and cruciate ligaments. The figure has been modified from ref. [6].	5
Figure 5: Schematic drawing of the flexion process and the according movement between femur and tibia. The figure has been modified from ref. [20].	6
Figure 6: Schematic of the tibial plateau from above. The change of the center of rotation of the femoral condyles during flexion of the knee is indicated. The lateral condyle performs a “roll-back” motion, while the medial condyle rotates around the same horizontal axis. This image has been modified from ref.[21].	7
Figure 7: Schematic of the displacement of the ACL as function of force applied to it, including the over-constraint and loose regions. This figure has been adapted from ref. [25].	8
Figure 8: <i>ACL tear type classification by Sherman et al. This figure has been modified from ref. [32].</i>	9
Figure 9: Possible treatments for an ACL injury.	10
Figure 10: Autograft options for an ACL reconstruction. This image has been modified from ref. [41].	12
Figure 11: 3D CT model of single bundle technique (left) and double bundle technique (right). This figure has been modified from ref. [43].	13
Figure 12: Most frequently used fixation devices: Adjustable loop device (A), fixed loop device (B), cross pin (C), and interference screw (D) The images shown in C & D have been modified from refs. [55, 56].	14
Figure 13: Hamstring autograft with ALD (TightRope, Arthrex, Naples, USA). This figure has been modified from ref. [57].	15
Figure 14: (A) shows the tunnels and sockets drilled into femur and tibia while (B) displays the socket and the intra-articular length. The figure has been modified from ref. [58].	15
Figure 15: ACL reconstruction using an ALD for the graft fixation; Panel A shows the graft passed through the femur while panel B shows the insertion of the graft into the tibia. The figure has been modified from ref.[59].	16
Figure 16: Five phases of the way to the market of a medical device [60].	16
Figure 17: Schematic of changes in directives and regulations: AIMD & MDD are replaced by MDR, IVD is replaced by IVDR [61].	17

Figure 18: The nine different groups of cortical fixation devices are presented. (A) RetroButton (Arthrex,USA), (B) EndoButton (Smith and Nephew, Great Britain), (C) GraftMax (ConMed Linvatec Inc., USA), (D) UltraButton (Smith and Nephew, London, Great Britain), (E) ProCinch (Stryker, USA), (F) ToggleLoc (Biomet, USA), (G) RigidLoop (Mitek Sports Medicine, DePuy Synthes, Switzerland), (H) TightRope II (Arthrex, Florida).....	20
Figure 19: Pictures of TightRope II (Arthrex, USA) (A) with marked interconnected loops and ProCinch (Stryker, USA) (B). Both devices have four strands.....	23
Figure 20: (A) Picture of the ALD ProCinch from Stryker with its two shortening strands, which need to be pulled alternating. (B) Picture of the ALD Rigidloop from DePuy Synthes, which has to be operated single-handedly. (C) Picture of the ALD ToggleLoc, with the antegrade shortening mechanism.	24
Figure 21: Pictures of the ALD GraftMax [71] and a medial cut of the button (B), this figure has been adapted from ref. [72].....	24
Figure 22: Picture of the ALD ProCinch (Stryker, USA) with its locking mechanism indicated (A) and schematic drawing of the function of the locking mechanism (B).	25
Figure 23: Picture of the test setup used for tensioning test.	27
Figure 24: Schematic representation of the loop shortening test process.	28
Figure 25: (A) Schematic drawing of the test setup for the stability single device test, the tested device is shown in black. (B) Picture of the test setup for the stability single device testing.	30
Figure 26: Testing protocol of the single device test with load and displacement on two x-axis, as functions of the time.	31
Figure 27: Pictures of the preparation steps for the bovine tendons for the stability tests. (A) Extraction of the extensor tendon. (B) Splitting the extracted tendon according to the black dashed line. (C) Pulling the folded tendon through a graft sizing block to measure the diameter. (D) Device tendon construct with initial stich. (E) Ends of the tendon including five whip-stiches. (F) Final device-tendon construct.....	32
Figure 28: (A) Schematic drawing of the stability test setup. (B) Pictures of the setup preparation for the device tendon test and picture of the final test (C).	33
Figure 29: Schematic drawing of the total bounce back.....	34
Figure 30: Schematic drawing of the force applied by the Instron to shorten the loop as function of the actual displacement of the machine actuator with attached suture clamp.	35
Figure 31: Illustration of the four phases and the respective main steps of the development process of TightRope II.	38
Figure 32: Flowchart of the possibilities for the conformity assessment for a class IIb medical device.	41
Figure 33: Flowchart of the conformity assessment procedure according to annex IX of MDR.....	42
Figure 34: Flowchart of the conformity assessment procedure according to Annex X and XI of MDR.	44

Figure 35: Picture of the non-polished (A) and polished (B) buttons of TightRope II.	44
Figure 36: Average total bounce back of the non-polished and polished version of TightRope II (Arthrex, USA) as a function of the load level. The shown values are the average of eight measurements and the error bars represent the standard deviation between those measurements.	45
Figure 37: Total displacement of the polished and non-polished version of TightRope II after cyclic loading for 3000 cycles. The shown values are the average of eight measurements and the error bars represent the standard deviation between those measurements.	46
Figure 38: Loop shortening in mm as a function of the load levels for the different testes ALD groups. The shown values are the average of eight measurements and the error bars represent the standard deviation between those measurements. The red line indicates the expected position after the shortening.	47
Figure 39: Pictures of the position of the button during the loop shortening, (A) RigidLoop, (B) GraftMax, (C & D) ProCinch. The blue arrow in panel D indicates the movement of the shortening suture toward the center.	48
Figure 40: Calculated total bounce back values as a function of the six load levels for the different devices. The shown values are the average of eight measurements and the error bars represent the standard deviation between those measurements.	49
Figure 41: Tensioning force as a function of the applied weight. The red line indicates a 1:1 transmission ratio. The shown values are the average of eight measurements and the error bars represent the standard deviation between those measurements.	50
Figure 42: Absolute displacement as a function of the cycles of loading and unloading for each tested group. The results of the single device test series are shown in grey and results of the device-tendon series in black. The red line indicates the clinical failure criteria of 3 mm.	52
Figure 43: Peak load at clinical failure as a function of the tested cycles. The results of GraftMax, ProCinch, ToggleLoc and Ultrabutton of the single device test are shown.	53
Figure 44: Peak load at clinical failure as a function of the tested cycles. The results of the ALDs GraftMax, ProCinch, ToggleLoc and UltraButton of the device-tendon tests are shown.	54

Tables

Table 1: Advantages and disadvantages of autografts. This table has been adapted from ref. [4].	12
Table 2: Overview over the design details of the analyzed ALDs, CFT (chinese finger trap). [65-70].	22
Table 3: List of the components used for the loop shortening tests are listed in this table.	26
Table 4: Weights applied to the loop and the according forces used for the preconditioning.	27
Table 5: Overview over the components used for the stability test.	29
Table 6: Overview of the mean values of the cycles of clinical failure and the according standard deviation cycles. Including the results of the single device test and of the Device-Tendon test.	54
Table 7: Results of the post hoc Tukey test of the cycles of clinical failure. The results for the single device test and for the device-tendon test are shown.	55
Table 8: Mean elongation and standard deviation of eight measurements. The results of the ALDs, that do not reach clinical failure and the FLDs after 3000 cycles of loading and complete unloading are shown.	55
Table 9: Results of the post hoc Tukey test for comparison of the elongation after 3000 cycles. The results for the single device tests and the device-tendon tests are shown.	56
Table 10: Overview over the mean values and the according standard deviation of the achieved loop shortening of the six tested ALD groups for the six load levels.	B
Table 11: The p-values of the post hoc Tukey tests are shown for all six tested load levels are presented.	B
Table 12: Overview over the mean \pm the standard deviation values for the total bounce back.	D
Table 13: The p-values of the post hoc Tukey tests of the total bounce back are shown for all six tested load levels are presented.	D
Table 14: Overview over the mean values and the according standard deviation of the force required to shorten the loops at the six tested load levels.	F
Table 15: The p-values of the post hoc Tukey tests of the tensioning are shown for all six tested load levels are presented.	F

Appendix

Appendix I: Results Statistical Analysis - Loop Shortening..... B
Appendix II: Results Statistical Analysis - Total Bounce Back..... D
Appendix II: Results Statistical Analysis – Tensioning..... F

B

Appendix I: Results Statistical Analysis - Loop Shortening

Table 10: Overview over the mean values and the according standard deviation of the achieved loop shortening of the six tested ALD groups for the six load levels.

load level in kg	mean ± SD of the loop shortening in mm					
	Graft-Max	Pro-Cinch	Rigid-Loop	Tight-Rope II	Toggle-Loc	Ultra-Button
1.5	11.23 ± 1.4	9.0 ± 0.3	10.1 ± 0.1	9.9 ± 0.3	8.8 ± 0.4	10.0 ± 0.2
3.5	9.9 ± 0.4	8.7 ± 0.3	9.9 ± 0.1	9.5 ± 0.2	7.7 ± 0.4	9.7 ± 0.2
5.5	9.3 ± 0.4	8.3 ± 0.4	9.8 ± 0.1	9.2 ± 0.2	7.4 ± 0.4	9.5 ± 0.2
7.5	8.7 ± 0.3	8.1 ± 0.2	9.7 ± 0.1	9.3 ± 0.2	7.2 ± 0.3	9.5 ± 0.2
9.5	8.5 ± 0.5	7.9 ± 0.4	9.7 ± 0.1	9.1 ± 0.2	7.1 ± 0.2	9.6 ± 0.1
15	8.0 ± 0.2	7.4 ± 0.4	9.6 ± 0.1	8.9 ± 0.3	6.7 ± 0.3	9.4 ± 0.1

Table 11: The p-values of the post hoc Tukey tests are shown for all six tested load levels are presented.

load level 1.5	GraftMax	ProCinch	RigidLoop	TightRope II	ToggleLoc	UltraButton
GraftMax	-	<0.001	0.012	0.003	<0.001	0.005
ProCinch	<0.001	-	0.035	0.110	0.005	0.069
RigidLoop	0.012	0.035	-	0.996	0.005	1
TightRope II	0.003	0.110	0.996	-	0.018	1
ToggleLoc	<0.001	0.973	0.005	0.018	-	0.010
UltraButton	0.005	0.069	1	1	0.010	-
load level 3.5	GraftMax	ProCinch	RigidLoop	TightRope II	ToggleLoc	UltraButton
GraftMax	-	<0.001	1	0.023	<0.001	0.726
ProCinch	<0.001	-	<0.001	<0.001	<0.001	<0.001
RigidLoop	1	<0.001	-	0.025	<0.001	0.743
TightRope II	0.023	<0.001	0.025	-	<0.001	0.423
ToggleLoc	<0.001	<0.001	<0.001	<0.001	-	<0.001
UltraButton	0.726	<0.001	0.743	0.423	<0.001	-

load level 5.5	GraftMax	ProCinch	RigidLoop	TightRope II	ToggleLoc	UltraButton
<i>GraftMax</i>	-	<0.001	0.001	0.986	<0.001	0.683
<i>ProCinch</i>	<0.001	-	<0.001	<0.001	<0.001	<0.001
<i>RigidLoop</i>	0.001	<0.001	-	0.002	<0.001	0.290
<i>TightRope II</i>	0.986		0.002	-	<0.001	0.294
<i>ToggleLoc</i>	<0.001	<0.001	<0.001	<0.001	-	<0.001
<i>UltraButton</i>	0.683	<0.001	0.290	0.294	<0.001	-
load level 7.5	GraftMax	ProCinch	RigidLoop	TightRope II	ToggleLoc	UltraButton
<i>GraftMax</i>	-		<0.001	<0.001	<0.001	<0.001
<i>ProCinch</i>	<0.001	-	<0.001	<0.001	<0.001	<0.001
<i>RigidLoop</i>	<0.001	<0.001	-	0.002	<0.001	0.498
<i>TightRope II</i>	<0.001	<0.001	0.002	-	<0.001	0.237
<i>ToggleLoc</i>	<0.001	<0.001	<0.001	<0.001	-	<0.001
<i>UltraButton</i>	<0.001	<0.001	0.498	0.237	<0.001	-
load level 9.5	GraftMax	ProCinch	RigidLoop	TightRope II	ToggleLoc	UltraButton
<i>GraftMax</i>	-	0.003	<0.001	<0.001	<0.001	<0.001
<i>ProCinch</i>	0.003	-	<0.001	<0.001	<0.001	<0.001
<i>RigidLoop</i>	<0.001	<0.001	-	0.002	<0.001	0.962
<i>TightRope II</i>	<0.001	<0.001	0.002	-	<0.001	0.019
<i>ToggleLoc</i>	<0.001	<0.001	<0.001	<0.001	-	<0.001
<i>UltraButton</i>	<0.001	<0.001	0.962	0.019	<0.001	-
load level 15	GraftMax	ProCinch	RigidLoop	TightRope II	ToggleLoc	UltraButton
<i>GraftMax</i>	-	<0.001	<0.001	<0.001	<0.001	<0.001
<i>ProCinch</i>	<0.001	-	<0.001	<0.001	<0.001	<0.001
<i>RigidLoop</i>	<0.001	<0.001	-	<0.001	<0.001	0.196
<i>TightRope II</i>	<0.001	<0.001	<0.001	-	<0.001	0.010
<i>ToggleLoc</i>	<0.001	<0.001	<0.001	<0.001	-	<0.001
<i>UltraButton</i>	<0.001	<0.001	0.196	0.010	<0.001	-

D

Appendix II: Results Statistical Analysis - Total Bounce Back

Table 12: Overview over the mean \pm the standard deviation values for the total bounce back.

load-level	mean \pm SD of the total bounce back in mm							
	Graft-Max	Pro-Cinch	Rigid-Loop	Tight-Rope II	Toggle-Loc	Ultra-Button	Endo-Button	Retro-Button
1.5	-8.7 \pm 0.9	-1.8 \pm 0.5	-1.7 \pm 0.1	-2.5 \pm 0.3	-1.7 \pm 0.3	-2.6 \pm 0.3	-0.56 \pm 0.08	-0.52 \pm 0.06
3.5	-6.2 \pm 0.3	-1.5 \pm 0.4	-1.4 \pm 0.1	-2.0 \pm 0.1	-0.9 \pm 0.1	-1.6 \pm 0.2	-0.43 \pm 0.07	-0.29 \pm 0.02
5.5	-5.4 \pm 0.3	-1.3 \pm 0.3	-1.2 \pm 0.1	-1.6 \pm 0.1	-0.5 \pm 0.1	-1.3 \pm 0.2	-0.31 \pm 0.04	-0.17 \pm 0.05
7.5	-4.7 \pm 0.3	-1.0 \pm 0.2	-1.0 \pm 0.6	-1.3 \pm 0.1	-0.3 \pm 0.1	-0.9 \pm 0.2	-0.2 \pm 0.02	-0.13 \pm 0.01
9.5	-4.3 \pm 0.4	-0.7 \pm 0.2	-1.0 \pm 0.1	-1.12 \pm 0.03	-0.26 \pm 0.03	-0.8 \pm 0.1	-0.03 \pm 0.03	-0.09 \pm 0.02
15	-3.5 \pm 0.2	-0.6 \pm 0.2	-0.8 \pm 0.1	-0.8 \pm 0.1	-0.037 \pm 0.02	-0.5 \pm 0.1	0.003 \pm 0.003	-0.004 \pm 0.003

Table 13: The p-values of the post hoc Tukey tests of the total bounce back are shown for all six tested load levels are presented.

load level	Graft-Max	Pro-Cinch	Rigid-Loop	Tight-Rope II	Toggle-Loc	Ultra-Button	Retro-Button	Endo-Button
1.5								
GraftMax	-	<0.001	<0.001	<0.001	<0.001	<0.001	<0.001	<0.001
ProCinch	<0.001	-	1	0.848	1	0.793	0.318	0.529
RigidLoop	<0.001	1	-	0.826	1	0.766	0.344	0.557
TightRope II	<0.001	0.848	0.826	-	0.824	1	0.011	0.047
ToggleLoc	<0.001	1	1	0.824	-	0.765	0.346	0.558
UltraButton	<0.001	0.793	0.766	1	0.756	-	0.008	0.037
RetroButton	<0.001	0.318	0.344	0.011	0.346	0.008	-	1
EndoButton	<0.001	0.529	0.557	0.047	0.558	0.037	1	-
3.5								
GraftMax	-	<0.001	<0.001	<0.001	<0.001	<0.001	<0.001	<0.001
ProCinch	<0.001	-	0.863	<0.001	<0.001	1	<0.001	<0.001
RigidLoop	<0.001	0.863	-	<0.001	<0.001	0.590	<0.001	<0.001
TightRope II	<0.001	<0.001	<0.001	-	<0.001	<0.001	<0.001	<0.001
ToggleLoc	<0.001	<0.001	<0.001	<0.001	-	<0.001	<0.001	0.005
UltraButton	<0.001	1	0.590	<0.001	<0.001	-	<0.001	<0.001
RetroButton	<0.001	<0.001	<0.001	<0.001	<0.001	<0.001	-	0.924
EndoButton	<0.001	<0.001	<0.001	<0.001	0.005	<0.001	0.924	-

load level 5.5	Graft-Max	Pro-Cinch	Rigid-Loop	Tight-Rope II	Toggle-Loc	Ultra-Button	Retro-Button	Endo-Button
GraftMax	-	<0.001	<0.001	<0.001	<0.001	<0.001	<0.001	<0.001
ProCinch	<0.001	-	0.999	0.014	<0.001	1	<0.001	<0.001
RigidLoop	<0.001	0.999	-	0.002	<0.001	0.983	<0.001	<0.001
TightRope II	<0.001	0.014	0.002	-	<0.001	0.035	<0.001	<0.001
ToggleLoc	<0.001	<0.001	<0.001	<0.001	-	<0.001	0.032	0.819
UltraButton	<0.001	1	0.983	0.035	<0.001	-	<0.001	<0.001
RetroButton	<0.001	<0.001	<0.001	<0.001	0.032	<0.001	-	0.831
EndoButton	<0.001	<0.001	<0.001	<0.001	0.819	<0.001	0.831	-
load level 7.5	Graft-Max	Pro-Cinch	Rigid-Loop	Tight-Rope II	Toggle-Loc	Ultra-Button	Retro-Button	Endo-Button
GraftMax	-	<0.001	<0.001	<0.001	<0.001	<0.001	<0.001	<0.001
ProCinch	<0.001	-	0.953	<0.001	<0.001	0.880	<0.001	<0.001
RigidLoop	<0.001	0.953	-	0.007	<0.001	0.244	<0.001	<0.001
TightRope II	<0.001	<0.001	0.007	-	<0.001	<0.001	<0.001	<0.001
ToggleLoc	<0.001	<0.001	<0.001	<0.001	-	<0.001	0.101	0.740
UltraButton	<0.001	0.880	0.244	<0.001	<0.001	-	<0.001	<0.001
RetroButton	<0.001	<0.001	<0.001	<0.001	0.101	<0.001	-	0.985
EndoButton	<0.001	<0.001	<0.001	<0.001	0.740	<0.001	0.985	-
load level 9.5	Graft-Max	Pro-Cinch	Rigid-Loop	Tight-Rope II	Toggle-Loc	Ultra-Button	Retro-Button	Endo-Button
GraftMax	-	<0.001	<0.001	<0.001	<0.001	<0.001	<0.001	<0.001
ProCinch	<0.001	-	0.003	<0.001	<0.001	0.573	<0.001	<0.001
RigidLoop	<0.001	0.003	-	0.924	<0.001	0.312	<0.001	<0.001
TightRope II	<0.001	<0.001	0.924	-	<0.001	0.019	<0.001	<0.001
ToggleLoc	<0.001	<0.001	<0.001	<0.001	-	<0.001	0.967	1
UltraButton	<0.001	0.573	0.312	0.019	<0.001	-	<0.001	<0.001
RetroButton	<0.001	<0.001	<0.001	<0.001	0.967	<0.001	-	0.999
EndoButton	<0.001	<0.001	<0.001	<0.001	1	<0.001	0.999	-
load level 15	Graft-Max	Pro-Cinch	Rigid-Loop	Tight-Rope II	Toggle-Loc	Ultra-Button	Retro-Button	Endo-Button
GraftMax	-	<0.001	<0.001	<0.001	<0.001	<0.001	<0.001	<0.001
ProCinch	<0.001	-	0.196	0.234	<0.001	0.860	<0.001	<0.001
RigidLoop	<0.001	0.196	-	1	<0.001	0.006	<0.001	<0.001
TightRope II	<0.001	0.234	1	-	<0.001	0.007	<0.001	<0.001
ToggleLoc	<0.001	<0.001	<0.001	<0.001	-	<0.001	1	1
UltraButton	<0.001	0.860	0.006	0.007	<0.001	-	<0.001	<0.001
RetroButton	<0.001	<0.001	<0.001	<0.001	1	<0.001	-	1
EndoButton	<0.001	<0.001	<0.001	<0.001	1	<0.001	1	-

Appendix II: Results Statistical Analysis – Tensioning

Table 14: Overview over the mean values and the according standard deviation of the force required to shorten the loops at the six tested load levels.

load level in kg	mean \pm SD tensioning force in N					
	GraftMax	ProCinch	RigidLoop	TightRope II	ToggleLoc	UltraButton
1.5	18.3 \pm 0.4	12.4 \pm 0.5	10.9 \pm 0.7	12.2 \pm 1.3	57.9 \pm 7.9	18.3 \pm 0.8
3.5	38.7 \pm 0.6	28.2 \pm 1.3	22.0 \pm 0.9	27.2 \pm 1.7	115.9 \pm 15.3	35.3 \pm 1,9
5.5	58.0 \pm 0.7	43.8 \pm 0.6	32.9 \pm 1.26	41.2 \pm 1.4	153.4 \pm 10.9	50.4 \pm 1.7
7.5	79.3 \pm 1.4	59.1 \pm 0.8	43.8 \pm 1.7	56.8 \pm 1.6	176.8 \pm 14.3	64.6 \pm 2.6
9.5	97.9 \pm 1.6	70.7 \pm 4.9	51.6 \pm 1.5	67.9 \pm 2.2	219.2 \pm 14.9	80.6 \pm 2.3
15	148.3 \pm 1.8	110.5 \pm 1.3	75.1 \pm 2.2	107.2 \pm 16.2	303.5 \pm 12.5	121.0 \pm 5.0

Table 15: The p-values of the post hoc Tukey tests of the tensioning are shown for all six tested load levels are presented.

load level 1.5	GraftMax	ProCinch	RigidLoop	TightRope II	ToggleLoc	UltraButton
GraftMax	-	0.011	<0.001	0.009	<0.001	1
ProCinch	0.011	-	0.941	1	<0.001	0.012
RigidLoop	<0.001	0.941	-	0.964	<0.001	<0.001
TightRope II	0.009	1	0.964	-	<0.001	0.009
ToggleLoc	<0.001	<0.001	<0.001	<0.001	-	<0.001
UltraButton	1	0.012	<0.001	0.009	<0.001	-
load level 3.5	GraftMax	ProCinch	RigidLoop	TightRope II	ToggleLoc	UltraButton
GraftMax	-	0.022	<0.001	0.012	<0.001	0.886
ProCinch	0.022	-	0.397	1	<0.001	0.247
RigidLoop	<0.001	0.397	-	0.536	<0.001	0.002
TightRope II	0.012	1	0.536	-	<0.001	0.161
ToggleLoc	<0.001	<0.001	<0.001	<0.001	-	<0.001
UltraButton	0.886	0.247	0.002	0.161	<0.001	-

load level 5.5	GraftMax	ProCinch	RigidLoop	TightRope II	ToggleLoc	UltraButton
<i>GraftMax</i>	-	<0.001	<0.001	<0.001	<0.001	0.023
<i>ProCinch</i>	<0.001	-	<0.001	0.860	<0.001	0.066
<i>RigidLoop</i>	<0.001	<0.001	-	0.010	<0.001	<0.001
<i>TightRope II</i>	<0.001	0.860	0.010	-	<0.001	0.003
<i>ToggleLoc</i>	<0.001	<0.001	<0.001	<0.001	-	<0.001
<i>UltraButton</i>	0.023	0.066	<0.001	0.003	<0.001	-
load level 7.5	GraftMax	ProCinch	RigidLoop	TightRope II	ToggleLoc	UltraButton
<i>GraftMax</i>	-	<0.001	<0.001	<0.001	<0.001	<0.001
<i>ProCinch</i>	<0.001	-	<0.001	0.841	<0.001	0.284
<i>RigidLoop</i>	<0.001	<0.001	-	0.005	<0.001	<0.001
<i>TightRope II</i>	<0.001	0.841	0.005	-	<0.001	0.021
<i>ToggleLoc</i>	<0.001	<0.001	<0.001	<0.001	-	<0.001
<i>UltraButton</i>	<0.001	0.284	<0.001	0.021	<0.001	-
load level 9.5	GraftMax	ProCinch	RigidLoop	TightRope II	ToggleLoc	UltraButton
<i>GraftMax</i>	-	<0.001	<0.001	<0.001	<0.001	<0.001
<i>ProCinch</i>	<0.001	-	<0.001	0.955	<0.001	0.049
<i>RigidLoop</i>	<0.001	<0.001	-	<0.001	<0.001	<0.001
<i>TightRope II</i>	<0.001	0.955	<0.001	-	<0.001	0.005
<i>ToggleLoc</i>	<0.001	<0.001	<0.001	<0.001	-	<0.001
<i>UltraButton</i>	<0.001	0.049	<0.001	0.005	<0.001	-
load level 15	GraftMax	ProCinch	RigidLoop	TightRope II	ToggleLoc	UltraButton
<i>GraftMax</i>	-	<0.001	<0.001	<0.001	<0.001	<0.001
<i>ProCinch</i>	<0.001	-	<0.001	0.972	<0.001	0.173
<i>RigidLoop</i>	<0.001	<0.001	-	<0.001	<0.001	<0.001
<i>TightRope II</i>	<0.001	0.972	<0.001	-	<0.001	0.031
<i>ToggleLoc</i>	<0.001	<0.001	<0.001	<0.001	-	<0.001
<i>UltraButton</i>	<0.001	0.173	<0.001	0.031	<0.001	-